An evaporated seawater origin for the ore-forming brines in unconformity-related uranium deposits (Athabasca Basin, Canada): Cl/Br and δ^{37}Cl analysis of fluid inclusions

Antonin Richard, David A Banks, Julien Mercadier, Marie-Christine Boiron, Michel Cuney, Michel Cathelineau

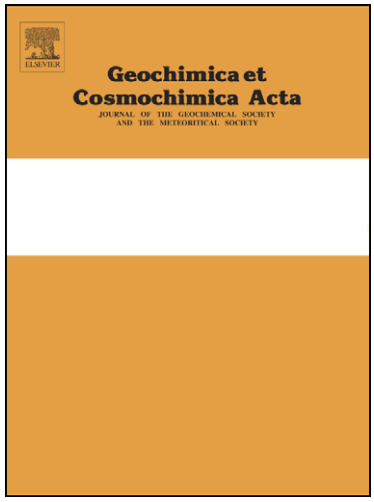

An evaporated seawater origin for the ore-forming brines in unconformity-related uranium deposits (Athabasca Basin, Canada): Cl/Br and δ ^{37}Cl analysis of fluid inclusions

Antonin Richard, David A. Banks, Julien Mercadier, Marie-Christine Boiron, Michel Cuney, Michel Cathelineau

PII: S0016-7037(11)00105-0
DOI: 10.1016/j.gca.2011.02.026
Reference: GCA 7105

To appear in: *Geochimica et Cosmochimica Acta*

Received Date: 16 July 2010
Accepted Date: 17 February 2011

Please cite this article as: Richard, A., Banks, D.A., Mercadier, J., Boiron, M-C., Cuney, M., Cathelineau, M., An evaporated seawater origin for the ore-forming brines in unconformity-related uranium deposits (Athabasca Basin, Canada): Cl/Br and δ ^{37}Cl analysis of fluid inclusions, *Geochimica et Cosmochimica Acta* (2011), doi: 10.1016/j.gca.2011.02.026

An evaporated seawater origin for the ore-forming brines in unconformity-related uranium deposits (Athabasca Basin, Canada): Cl/Br and $\delta^{37}Cl$ analysis of fluid inclusions

Antonin Richard[1*], David A. Banks[2], Julien Mercadier[1], Marie-Christine Boiron[1], Michel Cuney[1], Michel Cathelineau[1]

[1]G2R, Nancy-Université, CNRS, CREGU, Boulevard des Aiguillettes B.P. 70239, F-54506, Vandoeuvre-lès-Nancy, France

[2] School of Earth and Environment, University of Leeds, Woodhouse Lane, Leeds, LS2 9JT, UK

*Corresponding author: Antonin Richard, G2R, Nancy-Université, CNRS, CREGU, Boulevard des Aiguillettes B.P. 70239, F-54506, Vandoeuvre-lès-Nancy, France, Tel.: +33 3 83 68 47 25, Fax: 33 3 83 68 47 01, *E-mail address:* antonin.richard@g2r.uhp-nancy.fr (A. Richard).

Abstract

Analyses of halogen concentration and stable chlorine isotope composition of fluid inclusions from hydrothermal quartz and carbonate veins spatially and temporally associated with giant unconformity-related uranium deposits from the Paleoproterozoic Athabasca Basin (Canada) were performed in order to determine the origin of chloride in the ore-forming brines. Microthermometric analyses show that samples contain variable amounts of a NaCl-rich brine (Cl concentration between 120,000 to 180,000 ppm) and a $CaCl_2$-rich brine (Cl concentration between 160,000 to 220,000 ppm). Molar Cl/Br ratios of fluid inclusion

leachates range from ~100 to ~900, with most values between 150 and 350. Cl/Br ratios below 650 (seawater value) indicate that the high salinities were acquired by evaporation of seawater. Most $\delta^{37}Cl$ values are between -0.6 and 0‰ (seawater value) which is also compatible with a common evaporated seawater origin for both NaCl- and $CaCl_2$-rich brines.

Slight discrepancies between the Cl concentration, Cl/Br, $\delta^{37}Cl$ data and seawater evaporation trends, indicate that the evaporated seawater underwent secondary minor modification of its composition by: (i) mixing with a minor amount of halite-dissolution brine or re-equilibration with halite during burial; (ii) dilution in a maximum of 30% of connate and/or formation waters during its migration towards the base of the Athabasca sandstones; (iii) leaching of chloride from biotites within basement rocks and (iv) water loss by hydration reactions in alteration haloes linked to uranium deposition.

The chloride in uranium ore-forming brines of the Athabasca Basin has an unambiguous dominantly marine origin and has required large-scale seawater evaporation and evaporite deposition. Although the direct evidence for evaporative environments in the Athabasca Basin are lacking due to the erosion of ~80% of the sedimentary pile, Cl/Br ratios and $\delta^{37}Cl$ values of brines have behaved conservatively at the basin scale and throughout basin history.

1. INTRODUCTION

Chloride is an important metal-complexing agent in crustal fluids (Yardley, 2005). Numerous basin-hosted mineral deposits are thought to have formed from high chlorinity basinal brines where metal complexing by Cl was important. Examples include the Cu-Co from Zambian Copper Belt deposits (McGowan et al., 2006), Pb-Zn from MVT and extension-related deposits (Kesler et al., 1995; Muchez et al., 2005; Boiron et al., 2010) and

unconformity-related U deposits (Derome et al., 2005; Richard et al., 2010). Although the source of salinity is often distinct from that of metals, determining the origin and evolution of Cl in mineralizing fluids is of crucial importance for metallogenic models.

Cl/Br ratios and $\delta^{37}Cl$ compositions have been widely used as a tool for determining the origin of salinity in various present-day and ancient crustal fluids (e.g. Carpenter et al., 1974; Böhlke and Irwin, 1992; Eastoe and Guilbert, 1992; Fontes and Matray, 1993; Worden, 1996; Banks et al., 2000a, 2000b; Chiaradia et al., 2006; Nahnybida et al., 2009; Gleeson and Smith, 2009). Cl and to a lesser extent Br substitute for –OH in minerals (ionic size being a major control) or can be leached from minerals, but in fluid dominated systems the amount removed or released by minerals is small relative to the overall fluid budget and does not perturb their concentration in the fluid to any large extent, resulting in distinctive Cl/Br ratios. Because Cl is the dominant anion of basinal brines and their Cl/Br and $\delta^{37}Cl$ systematics should reflect the mechanism(s) of acquisition of high salinities. Cl from basinal brines generally has a marine origin and chlorinity variations are mostly interpreted in terms of seawater evaporation, dissolution of evaporites and dilution by meteoric waters or seawater (Hanor, 1994).

Here, we present the Cl/Br and $\delta^{37}Cl$ systematics of diagenetic brines from the Paleoproterozoic Athabasca Basin (Saskatchewan, Canada). These 25-35 wt% eq. NaCl and 120-200°C brines are thought to have circulated over large distances at the basement-cover interface (Pagel, 1975). Along their migration path, the brines underwent significant fluid-rock interactions with the basin and basement lithologies and have mobilized large quantities of metals, especially U (Richard et al., 2010). Uranium was then deposited as giant unconformity-related type deposits (Kyser and Cuney, 2008). These brines are common as fluid inclusions located in quartz overgrowths in basin sandstones or in quartz-carbonate veins crosscutting basin sandstones and basement rocks. Microthermometry, Laser Induced

Breakdown Spectroscopy (LIBS), Raman spectroscopy and Laser Ablation-Inductively Coupled Plasma-Mass Spectrometry (LA-ICP-MS) analysis of these fluid inclusions showed that the composition of the brines varies from Na-Ca-Mg- to a Ca-Mg-Na-dominated cation composition (Derome et al., 2005; Richard et al., 2010). Large variations in major element concentrations were interpreted as resulting from mixing between a NaCl-rich and a $CaCl_2$-rich end-member. Both brines show important salinity variations, mainly in the 25-35 wt% eq. NaCl range, the $CaCl_2$-rich brine being generally more saline than the NaCl-rich brine (Derome et al., 2005). Because Cl is by far the most important anion in the Athabasca brines, it has been proposed to be one of the main potential U-complexing agents (Raffensperger and Garven, 1995a; Komninou and Sverjensky, 1996).

To learn more about the source of the brines, we have targeted five unconformity-related U deposits (McArthur River, Rabbit Lake, Eagle Point, P-Patch and Millennium) located in various parts of the Athabasca Basin (Fig. 1). It is noteworthy that, in their pioneer work on $\delta^{37}Cl$ variations of fluids in hydrothermal systems, Eastoe and Guilbert (1992) mentioned the potential usefulness of stable chlorine isotopes to determine the origin of high salinity brines in the Athabasca Basin. Since then, no study has been undertaken, using this technique, on the Athabasca brines.

Here, we attempted to answer the following questions: (i) What is the process responsible for the high salinity and the origin of high Cl concentrations in the Athabasca Basin brines? (ii) Is there a difference in the origin of Cl in the NaCl-rich and $CaCl_2$-rich brines? (iii) What is the explanation for the slight but systematic differences in chlorinity between the NaCl-rich and $CaCl_2$-rich brines? (iv) Is there any evidence for a non-marine Cl input (i.e. Cl from biotites-amphiboles) in the Athabasca Basin brines?

2. PREVIOUS STUDIES

Previous Cl/Br data for quartz and carbonate-hosted fluid inclusions in unconformity-related uranium deposits are sparse and hotly debated. Pagel and Jaffrezic (1977) used neutron activation to obtain Cl/Br ratios of fluid inclusion leachates from 11 quartz and dolomite veins from the Rabbit Lake deposit. They found molar Cl/Br ratios between 110 and 160. Pagel and Jaffrezic (1977) and Pagel et al., (1980) pointed out the lack of preserved evaporites in the area and interpreted these low Cl/Br ratios as resulting from catagenesis of organic matter, Br being easily substituted for hydrogen in organic compounds. More recently, Derome et al., (2005) used crush-leach techniques similar to those described in this study to show that fluid inclusions leachates from the McArthur River deposit containing both NaCl-rich and $CaCl_2$-rich brine inclusions have Cl/Br ratios ranging from 120 to 220, which is compatible with data from Pagel and Jaffrezic (1977). The authors argued that catagenesis of organic matter is not a process capable of fractionating Cl/Br ratios, especially in the case of the Athabasca Basin where organic matter is lacking. Finally, they interpreted the low Cl/Br ratios as resulting from evaporation of seawater beyond halite saturation, and stated that both brines share a common evaporated seawater origin.

The Kombolgie sub-Basin (McArthur Basin), Northern Territory, Australia, hosts very similar unconformity-related uranium deposits that were formed from comparable NaCl-rich and $CaCl_2$-rich brines (Wilde et al., 1989; Ypma and Fuzikawa, 1980; Derome et al., 2003, 2007; Polito et al., 2004, 2005). Continuing their use of crush-leach techniques, Derome et al., (2007) found molar Cl/Br ratios between 151 and 220 in fluid inclusion leachates from quartz veins. They argued that organic matter is nearly absent in the basin and in the basement and interpreted the low Cl/Br ratios as resulting from evaporation of seawater beyond halite saturation.

The origin of brines in the Athabasca Basin has also previously been discussed on the basis of the stable isotope (O, H) composition of alteration minerals. However, $\delta^{18}O$ and δD do not behave conservatively in hydrothermal systems and speculations on the origin of high chlorinities based only on $\delta^{18}O$ and δD of alterations minerals are highly questionable and lead to the following contradictory interpretations. Bray et al., (1988) suggested that $\delta^{18}O$ and δD compositions of the fluids in equilibrium with alteration minerals are incompatible with evaporation of seawater. The authors concluded that the high chlorinities were acquired by evaporite dissolution and that diagenesis of organic matter in shales could account for low Cl/Br ratios determined by Pagel and Jaffrezic (1977). Similarly, Kotzer and Kyser (1995) concluded that the brines have a significant meteoric water component and that the high chlorinities were achieved by evaporite dissolution and reaction with feldspars. However, based on comparable isotopic analyses, Alexandre et al., (2005) stated that the brines result from mixing between evaporated seawater and low-latitude meteoric waters.

3. BACKGROUND GEOLOGY AND SAMPLING

3.1. Regional geology

The Athabasca Basin lies on an Archean to Paleoproterozoic basement complex separated by the Northeast-trending Snowbird tectonic zone into two provinces, the Rae Province in the west and the Hearne Province in the east (Hoffman, 1990; Card et al., 2007) (Fig. 1). These two provinces consist of Archean gneisses, Paleoproterozoic metapelites and mafic to felsic intrusions, and were affected respectively by the ~2.0 to ~1.9 Ga Thelon-Talston and the ~1.9 to ~1.8 Ga Trans-Hudson orogenies (Card, 2002; Card et al., 2003; Chiarenzelli et al., 1998; Annesley et al., 2005). Most of the unconformity-related uranium

deposits of the Athabasca Basin, including those presented in this paper are located in the vicinity of the transition between two lithostructural domains of the Hearne Province, known as the Wollaston-Mudjatic transition zone (WMTZ) that consists of a Northeast-trending, anastomosing structure of Hudsonian age (1.8 Ga) (Annesley et al., 2005).

The sedimentary sequence of the Athabasca Basin, known as the Athabasca Group, unconformably overlies the crystalline basement and was deposited starting from 1.76 Ga (Ramaekers et al., 2007) (Fig. 1). The current maximum thickness of the sedimentary cover is ~1.5 km (Rumple Lake) and is thought to have reached ~5 km based on P-T estimations from fluid inclusion studies (Pagel, 1975; Derome et al., 2005). From the base to the top, the Athabasca Group is composed of fluvial to marginal marine quartz-rich sandstones of the Fair Point and Manitou Falls Formations, marine sandstones, phosphatic siltstones, and phosphatic mudstones of the Lazenby Lake and Wolverine Point Formations, sandstones of the Locker Lake and Otherside Formations, shales of the Douglas Formation and finally stromatolitic carbonates of the Carswell Formation (Ramaekers et al., 2007). The Douglas and Carswell formations are only preserved around the Carswell structure, which is thought to be the result of a meteorite impact (Pagel et al., 1985).

3.2. Unconformity-related U deposits

Due to their extremely high grade and tonnage, unconformity-related uranium deposits have accounted for more than 33% of the world's uranium production over the last 10 years (up to 192,000 tonnes U at 22% for the McArthur River deposit, Athabasca Basin) (Jefferson et al., 2007). Most of these deposits occur in the Paleoproterozoic intracratonic Athabasca Basin, Saskatchewan, Canada and in the Kombolgie sub-Basin, Northern Territory, Australia. In both basins, the ore is generally located close to the unconformity between the Archean to

Paleoproterozoic basement and the Paleoproterozoic sedimentary cover, and structurally controlled by basement-rooted graphite-rich faults. The spatial distribution of the ore and alteration minerals around the unconformity are highly variable from one deposit to another, suggesting different possible ore-forming fluid regimes (Quirt et al., 2003). Uranium mineralization can be strictly basement-hosted (e.g. P-Patch, Eagle Point and Millennium), unconformity-hosted (e.g. McArthur River, Rabbit Lake) or even sandstone-hosted (e.g. Cigar Lake).

The earliest unconformity-related U mineralizing events in the Athabasca Basin are dated between 1.5 and 1.4 Ga and various successive later episodes of mineralization and/or recrystallisation occurred between 1.4 Ga and 0.8 Ga (Cummings and Krstic, 1992; Fayek et al., 2002; Alexandre et al., 2009). Remobilization of primary U-ores is thought to have occurred nearly up to the present time (Mercadier et al., 2011).

The main alteration features associated with U-ores include in chronological order: (i) partial to complete replacement of the initial basement minerals (K-feldspar, biotite, plagioclase) by an illite + sudoite ± dravite assemblage as well as the precipitation of illite and sudoite in sandstones; (ii) dissolution of the basement and detrital quartz; (iii) dravite + quartz + uraninite + dolomite filling quartz dissolution vugs, veins, and breccias (Mercadier, 2008).

The most commonly accepted models for the formation of unconformity-related uranium deposits involve the interaction between oxidizing basinal brines and a basement-derived reducing fluid and/or reduced basement lithologies (Pagel and Jaffrezic, 1977; Hoeve and Sibbald, 1978; Pagel et al., 1980; Hoeve and Quirt, 1984; Wilson and Kyser, 1987; Kotzer and Kyser, 1995; Komninou and Sverjensky, 1996; Fayek and Kyser, 1997; Derome et al., 2003; 2005). Uranium is thought to be leached by the oxidizing basinal brines from accessory minerals and uranium oxides either in the basin (Fayek and Kyser, 1997, Kyser et al., 2000) or in the basement (Pagel et al., 1980; Annesley and Madore, 1999; Hecht and

Cuney, 2000; Madore et al., 2000). More recently, Derome et al., (2005) and Richard et al., (2010) pointed out the spatial and temporal relationship between U-ore and brine mixing, which suggests that mixing between U-bearing NaCl-rich and $CaCl_2$-rich brines could be a driving force for U deposition. Both brines originate from the basin and have strongly interacted with basement rocks, as shown by their elevated U concentrations (up to hundreds of ppm) (Richard et al., 2010).

3.3. Sampling

Quartz and carbonate veins are unambiguously genetically associated with the formation of the deposits and are likely to host fluid inclusions that are relicts of fluids responsible for the major alteration and mineralization events (Pagel et al., 1980; Kotzer and Kyser, 1995; Kyser et al., 2000; Derome et al., 2005; Richard et al., 2010). The quartz veins are clearly associated with the main stage of uranium deposition while carbonate veins are mostly found in late-ore paragenesis (see detailed description in Derome et al., 2005).

Sampling was essentially focused on specimens from the basement rocks for the following reasons: (i) fluid-rock interactions in the basement are thought to have drastically affected the composition of the brines (Derome et al., 2005; Mercadier et al., 2010; Richard et al., 2010); (ii) lack of preserved sedimentary cover at Rabbit Lake and Eagle Point precludes sampling in sandstones; (iii) no quartz or carbonate veins were observed in sandstones at P-Patch. For basement-hosted samples (27 quartz veins and 12 carbonate veins), the depth below the unconformity ranges from 21.6 m (DDH197.2, Rabbit Lake) to 360.7 m (EPE44.4, Eagle Point). Two quartz veins were sampled in sandstones at McArthur River (MAC13Qz, MAC8Qz).

Fig. 2 shows some typical quartz and carbonate veins studied in this work. The veins crosscut various lithologies such as gneisses or pegmatoids. Veins were sampled in relatively unaltered to fully altered (bleached) lithologies and can be filled by any of the following assemblages: dravite + quartz; quartz + dolomite ± bitumen ± pyrite; quartz only; dolomite ± hematite.

3.4. Summary of fluid inclusion data

Here, we present a brief summary of fluid inclusion data obtained for the studied samples. The complete description of fluid inclusion data for the studied deposits and a detailed discussion of their significance and implication for PTX conditions of fluid circulations around unconformity-related U deposits are presented in Derome et al., (2005), Richard (2009) and Richard et al., (2010).

In quartz and carbonate veins, mainly 5 to 25 µm two phase (liquid + vapor) and three phase (liquid + vapor + halite) fluid inclusions were observed (Fig. 2). The volumetric fraction of the vapor phase is between 5 and 15% with maximum frequency around 10%. A minor amount of inclusions contain solids with the presence of hematite and/or phyllosilicates, both interpreted as daughter minerals due to their relatively constant volume compared to the volume of fluid inclusions. They have negative crystal or more irregular shape and are found either along growth bands of the host mineral, as clusters of fluid inclusions, or as isolated inclusions. Therefore, the petrographic evidence suggests that the brine inclusions are either primary or pseudosecondary and coeval with the formation of their host minerals. Very minor amounts of low-salinity secondary inclusions similar to those described in Derome et al., (2005) are present and could not account for significant Cl and Br

248 contribution. Therefore, the samples are suitable for bulk extraction of fluid inclusions of
249 NaCl-rich and/or $CaCl_2$-rich brine type.

250 Microthermometry was carried out on fluid inclusions using a Linkam MDS600
251 heating-cooling stage. The temperatures of phase changes were measured for the following:
252 eutectic melting (Te), ice melting (Tm ice), hydrohalite melting (Tm hyd), halite dissolution
253 (Ts NaCl) and total homogenization (Th). According to the calibration curves, temperatures
254 of phase changes are given with an accuracy of about ± 5°C for Te, ± 0.1°C for Tm ice and
255 Tm hyd, and ± 1°C for Ts NaCl and Th.

256 Microthermometric observations have shown that the samples analyzed here contain
257 variable amounts of the NaCl-rich brine and $CaCl_2$-rich brine. The two brines are represented
258 by five fluid inclusion types, defined from their distinctive microthermometric behavior, by
259 Derome et al., (2005) for McArthur River and by Richard (2009) for the Eagle Point, Rabbit
260 Lake, P-Patch and Millennium deposits (Table 1). Inclusions showing a halite cube at room
261 temperature are noted Lwh' or Lwh according to the nature of the last phase to melt (ice or
262 hydrohalite respectively). Inclusions with no halite cube whose last phase to melt is
263 hydrohalite are noted Lw2. Inclusions with no halite cube whose last phase to melt is ice are
264 noted Lw' (-60°C < Tm ice < -30°C), Lw1 (-30°C < Tm ice < -15°C). After Derome et al.,
265 (2005) and Richard et al., (2010), Lw1, Lw2 and Lwh inclusions are representative of the
266 NaCl-rich brine and Lw' and Lwh' inclusions are representative of the $CaCl_2$-rich brine. All
267 inclusions homogenize to the liquid phase predominantly between 110 and 135°C, indicating
268 temperatures of fluid circulation of 120-200°C after pressure correction (Derome et al., 2005;
269 Richard et al., 2010). Based on microthermometric observations, an estimation of the relative
270 proportions of the two brines in each sample is reported in Table 2.

271 After microthermometric measurements and assuming that the brines are nearly pure
272 chloride salt solutions, the Cl concentrations in NaCl-rich brine inclusions range from

120,000 to 180,000 ppm and are centred on 150,000 ppm. $CaCl_2$-rich brine inclusions have Cl concentrations ranging from 160,000 to 220,000 ppm and centred on 190,000 ppm.

Further interpretation of Cl/Br and $\delta^{37}Cl$ data must take into account the contrasting salinities of the two brines and the fact that the analyzed solutions predominantly represent various contributions of the two brines.

4. ANALYTICAL METHODS

4.1. Cl-Br-F-SO_4 concentrations in fluid inclusions

Cl, Br, F and SO_4 concentrations were determined at the School of Earth and Environment, University of Leeds, UK, using the bulk crush-leach technique described in Banks and Yardley, (1992); Banks et al., (2000b) and Gleeson (2003). Quartz and carbonate veins were crushed to a grain size fraction of 1-2 mm. Pure mineral separates were then picked under a binocular microscope and placed in a ultrasonic bath for 1 hour. Then samples were cleaned by boiling twice in double distilled water. Cleaned quartz and carbonate grains (0.5 to 1.5 g) were then crushed to a fine powder in an agate pestle and mortar and leached in 5-6 ml of double distilled water. Leachates from fluid inclusions were analyzed for F, Cl, Br, and SO_4 with a Dionex DX-500 ion chromatograph. HCO_3 or CO_3 may also be present in the fluid inclusions (dolomite or calcite samples) but the ion chromatograph uses a carbonate eluent making their quantification impossible. The detection limit for the anions in fluid inclusion leachates was ~3 ppb for Cl and SO_4 and ~1 ppb for Br. Molar Cl/Br ratios are quoted with an error of less than ± 5% based on the replicate analysis of a standard seawater sample (Ocean Scientific GPS-1, Atlantic seawater).

Absolute Cl, Br, F and SO_4 concentrations of bulk fluid inclusion populations in individual samples were calculated using the average Cl content of fluid inclusion in each samples combined with the Cl/Br, Cl/F and Cl/SO_4 ratios, following the method for cations using Na determined from microthermometry (Banks et al., 2000b). However here we determine anions using the Cl value from microthermometry instead. There is obviously one unknown, but probably significant, uncertainty in the estimation of the average Cl content of bulk fluid inclusion populations in the analyzed samples, which is therefore quoted with an error of ± 10%.

4.2. Stable chlorine isotope analysis of fluid inclusions

A minimum of 0.1 mg of Cl is necessary for successful δ^{37}Cl determination, therefore only fluid inclusion leachates containing more than this were analyzed for ^{35}Cl and ^{37}Cl. This was based on the ion chromatographic determination of the Cl concentration in the leachates and the volume of that solution available. Cl was isolated as pure AgCl precipitate by addition of 4 ml of 1M KNO_3 and 2 ml of 5% (v/v) HNO_3, to a suitable volume of the leachate and heating to 85°C in an oven. Then 1 ml of 0.5M $AgNO_3$ was added to precipitate AgCl. The solution was filtered through a pre-weighed Whatman glass fiber filter paper, and the beaker and filter paper washed with 0.2% HNO_3, dried, re-weighed and the amount of AgCl determined. The papers were sealed in amber reaction bottles sealed with a septum top and wrapped in aluminium foil. Stable chlorine isotopes analysis, via continuous-flow isotope ratio mass spectrometry using a multicollector GV Instruments Isoprime™ IRMS, was carried out at the Stable Isotope Hydrology and Ecology Laboratory of Environment Canada in Saskatoon (Saskatchewan, Canada) following the methodology described in Wassenaar and Koehler, (2004). Stable chlorine isotope compositions were reported as δ^{37}Cl values in

standard per mil (‰) notation relative to SMOC (Standard Mean Ocean Chlorine) and are quoted with an error of ± 0.06‰ (1σ) based on repeated injections of 100% CH_3Cl.

4.3. Cl concentration in rocks and minerals

The Cl content and loss on ignition (L.O.I.) of fresh and altered pegmatites (P-Patch deposit) and porphyry granites (Eagle Point deposit) were determined from whole-rock geochemical analysis (SARM-CRPG, Nancy, France). In order to take into account the density modifications linked to hydrothermal alterations and to compare the samples at constant volume (i.e. to avoid the cavity volume), the density correction described in the following, is applied to all the altered samples, using the reference density of the freshest sample for each lithology. If d_1 and d_2 are the densities of the altered and freshest sample respectively, element concentrations of the altered sample are multiplied by d_1/d_2. These new concentrations allow proper comparison of samples with different degrees of alteration ("constant volume" correction).

The Cl concentrations in biotites from fresh porphyry granites (Eagle Point deposit) and illite and sudoite from altered porphyry granites (Eagle Point deposit) were measured by electron microprobe CAMECA SX100 (SCMEM laboratory, Nancy, France).

5. RESULTS

The reconstructed anion concentration in bulk fluid inclusion populations are shown in Table 2. Chloride is between 158,000 and 186,000 ppm and is by far the dominant anion. Br is between 409 and 4,350 ppm. F is frequently below detection limits but, when detected, is between 105 and 7,430 ppm. SO_4 is also frequently below the detection limit but, when

detected is between 206 and 8,200 ppm. Therefore, the Athabasca brines are effectively nearly pure chloride-salt solutions. Molar Cl/Br ratios are between 95 (the lowest Cl/Br ratio with 1,360 ppm more Br than any other sample) and 573 at Eagle Point, 151 and 224 at McArthur River, 333 and 892 at Millennium, 295 and 860 at P-Patch, 127 and 981 at Rabbit Lake. The most frequent Cl/Br ratios are between 100 and 300. Cl/Br ratios seem to be heterogeneously distributed in the different deposits, but the significance of these variations is questionable due to the relatively small number of samples for each deposits. For the Rabbit Lake deposit, the average Cl content of bulk fluid inclusion populations in carbonate veins is generally 5% less than in quartz veins, which should be related to a lesser relative abundance Lwh or Lwh' inclusions. Cl, Br, F, and SO_4 concentrations as well as Cl/Br ratios show no relationship with depth below the unconformity and lithology.

$\delta^{37}Cl$ values are between -1.08 and +0.79‰ with most values between -0.6 and 0‰ (seawater value) (Table 2). Only three $\delta^{37}Cl$ values are above 0‰. All the studied deposits show a mode of $\delta^{37}Cl$ values between -0.5 and 0‰. $\delta^{37}Cl$ values seem to be distributed equally among host minerals and brine contents. $\delta^{37}Cl$ values show no relationship with depth below unconformity.

Table 3 shows that the Cl content of fresh biotites from basement rocks are quite homogeneous and lie in the 3,200-4,200 ppm range. In altered rocks, biotites are completely altered to illite and sudoite, whose Cl content is from 210 to 340 ppm and 250 to 530 ppm respectively. The analyses of whole rocks show that the Cl content of fresh porphyries and pegmatites is from 215 to 343 ppm and 460 to 1,078 ppm, respectively. In altered porphyries and pegmatites, Cl is from 91 to 207 ppm and 67 to 298 ppm, respectively. The intensity of alteration can be estimated using loss on ignition values (L.O.I.). Fresh rocks have L.O.I. from 1.2 to 1.7 wt.% while altered rocks have L.O.I. from 1.5 to 9.4 wt.%.

6. DISCUSSION

6.1. Major influences on chlorinity, Cl/Br and δ^{37}Cl values

6.1.1. Past vs. present-day Cl/Br and δ^{37}Cl values of seawater

The molar Cl/Br ratio of seawater has evolved through the ages and was of ~450 in the Archean and Paleoproterozoic, and closer to 650 from Mesoproterozoic to the present time (De Ronde et al., 1997; Channer et al., 1997; Banks et al., 2003; Foriel et al., 2004). Thus, we assume that the Cl/Br ratio of seawater during the formation of unconformity-related uranium deposits in the Athabasca Basin (~1.4 Ga) was close to the present-day value. During evaporation of seawater and crystallization of halite, Br is preferentially partitioned into the fluid phase, resulting in Br-enriched residual brines, with Cl/Br ratios lower than that of seawater. Basinal fluids with Cl/Br ratios lower than that of seawater are thus typically derived from evaporation of seawater (Fontes and Matray, 1993 and references therein).

In the absence of available δ^{37}Cl values for past seawater and similarly to Cl/Br ratios, we assume that the δ^{37}Cl of Mesoproterozoic seawater was close to that of present-day value. The δ^{37}Cl signature of evaporated seawater is known experimentally from Eggenkamp et al., (1995) and Eastoe et al., (1999). Both studies led to comparable results. During evaporation of seawater up to epsomite saturation, δ^{37}Cl decreases in the residual brines from 0‰ (seawater) down to -0.5‰ after Eggenkamp et al., (1995) and down to -0.9‰ after Eastoe et al., (1999).

394 *6.1.2. A common evaporated seawater origin for NaCl- and $CaCl_2$-rich brines*

395

396 Here, the majority of Cl/Br ratios are lower than 300 with chlorinity ranging from
397 150,000 to 180,000 ppm, which is compatible with evaporated seawater beyond halite
398 saturation and close to epsomite or sylvite saturation (Fig. 3). In addition, most $\delta^{37}Cl$ values
399 are between -0.9 and 0‰ which is also compatible with evaporated seawater beyond halite
400 saturation. Although Cl/Br and $\delta^{37}Cl$ values may have been modified after seawater
401 evaporation (see below), possible chlorinity, Cl/Br and are $\delta^{37}Cl$ values of the initial halite to
402 sylvite-saturated evaporated seawater can reasonably be defined as follows: (i) Cl
403 concentration between 150,000 to 180,000 ppm; (ii) Cl/Br ratio between 100 and 300; (iii)
404 $\delta^{37}Cl$ values between 0 and -0.9‰ (Fig. 3, Fig. 4).

405 An important observation is that no relation can be observed between the relative
406 proportions of the NaCl-rich and $CaCl_2$-rich brines and the Cl/Br ratios and $\delta^{37}Cl$ values of
407 fluid inclusion leachates (Table 2). Although the brines have different dominant cations, the
408 data strongly indicate that both brines have comparable Cl/Br ratios and $\delta^{37}Cl$ signatures and
409 therefore share a common evaporated seawater origin.

410

411 *6.1.3. Why is no continental evaporitic brine involved?*

412

413 Continental evaporitic brines have highly variable compositions due to multiple
414 possible water inputs (mainly river and ground waters) (Risacher et al., 2003). The Cl/Br ratio
415 of river waters is comparable to that of seawater but if river water is mixed with groundwater
416 before onset of evaporation, the initial Cl/Br of the evaporating solution may considerably
417 differ from that of seawater. Further, Risacher et al., (2006) have shown that Br can display
418 non-conservative behaviour in surface waters and brines of Central Andes. Indeed, surface

419 waters at salar de Uyuni, Bolivia, are systematically Br-depleted and the authors suggest that
420 the missing Br was transferred into the atmosphere. The stable chlorine isotopic composition
421 of salt lake brines are known from Liu et al., (1997) and range from -2.05 to 1.01‰. Thus,
422 due to their high variability in continental environments Cl/Br and $\delta^{37}Cl$ signatures cannot
423 uniquely identify a continental origin for the brine. Finally, one of the main points against an
424 evaporated continental water as source of the Athabasca brines is that continental water has
425 very low initial Cl and Br concentrations compared to seawater. Therefore, to achieve the
426 observed high salinities would require the loss of almost all of the water from the evaporating
427 continental water, which could hardly account for the huge volume of brines involved in the
428 formation of unconformity-related uranium deposits throughout the Athabasca Basin.
429
430 *6.1.4. Insights from Cl/Br vs. $\delta^{37}Cl$ relationships*
431
432 The $\delta^{37}Cl$ signature of evaporated seawater determined by Eggenkamp et al., (1995)
433 and Eastoe et al., (1999) and Cl/Br ratios of evaporated seawater from Fontes and Matray
434 (1993) were combined and the resulting field for evaporated seawater was plotted with
435 analytical data in a Cl/Br vs. $\delta^{37}Cl$ diagram (Fig. 4). Some of the samples lie remote from the
436 field for evaporated seawater, which could be explained by subsequent modification of Cl/Br
437 and $\delta^{37}Cl$ values of the initial evaporated seawater during migration in the basin and/or
438 basement. Although the chlorinity, Cl/Br and $\delta^{37}Cl$ values of the initial evaporated seawater
439 are tightly constrained, additional minor factors may have subsequently influenced chlorinity,
440 Cl/Br and $\delta^{37}Cl$ values of the initial evaporated seawater. These factors are discussed below.
441

442 **6.2. Possible minor influences on chlorinity, Cl/Br and $\delta^{37}Cl$ values**

443

444 *6.2.1. Mixing between evaporated seawater and halite-dissolution brine*

445

446 Here, we consider the scenario of mixing between halite-to-carnallite-saturated
447 evaporated seawater, and halite-dissolution brine (Chi and Savard, 1997; Banks et al., 2000b;
448 Grandia et al., 2003a). Regardless of the origin of the fluid that dissolves halite (meteoric
449 water or seawater or a mixture of both), halite-dissolution brines are nearly pure NaCl-H_2O
450 solutions with chlorinity controlled by the solubility of halite, the fluid temperature and flow
451 rate. Halite-dissolution brines are Br-depleted compared to seawater with highly variable
452 Cl/Br ratios that should tend to that of the dissolved halite bodies (generally about 20,000). In
453 practice, halite recrystallization following dissolution is frequent and tends to lower the Cl/Br
454 ratio of the resulting brine (Banks et al., 2000b).

455 If the hypothetical dissolution of halite occurred at ~100°C halite solubility at 100°C
456 would constrain the chlorinity of the halite-dissolution brines to ~170,000 ppm (Bodnar,
457 1994). The Cl/Br ratio of halite-dissolution brines is set to 4,000 which is a lower estimate of
458 the possible Cl/Br ratio of these fluids. Fig. 5 shows mixing trends between a hypothetical
459 halite-dissolution brine (as defined above), and halite-to-carnallite-saturated evaporated
460 seawater. A contribution of 50% up to 90% from halite-dissolution fluid could account for the
461 majority of the measured Cl/Br ratios as seen in Fig. 3. This scenario maximizes the
462 contribution of halite-dissolution brine because its initial Cl/Br ratio is a lower estimate.
463 Therefore, the contribution of halite-dissolution brines is probably less than 50%. It is
464 expected that samples exhibiting the highest Cl/Br have the lowest Br contents, the Cl
465 concentration being pretty constant among samples. Also, evaporated seawater and halite-

466 dissolution brines have comparable Cl content. Therefore, their mixing is visible from Br
467 content only.

468 Recrystallization or dissolution does not affect the $\delta^{37}Cl$ of halite bodies (Eastoe and
469 Peryt, 1999) and thus the $\delta^{37}Cl$ signature of the halite-dissolution brine should reflect that of
470 the dissolved halite at the time of its deposition. Phanerozoic marine halites have $\delta^{37}Cl$
471 between -0.5 and +0.5‰ (Eastoe et al., 2007). Fig. 4 shows the possible trend of evaporated
472 seawaters that are the most likely to have been significantly affected by mixing with a minor
473 proportion of halite-dissolution brines.

474

475 *6.2.2. Re-equilibration between brine and halite*

476

477 During evaporation of seawater and subsequent precipitation of halite, the residual
478 brine can either percolate through the sedimentary pile or is trapped as fluid inclusions within
479 halite, the porosity of which can reach ~40% (Warren, 2010). Therefore, evaporites can
480 potentially trap large volumes of brines that can be expelled later due to compaction during
481 burial. Residual brines can be preserved with low Cl/Br ratios within evaporites even after
482 burial and unroofing (Fontes and Matray, 1993).

483 During burial and subsequent heating, significant re-equilibration between the residual
484 brines trapped as fluid inclusions and their host halite, is expected due to increasing halite
485 solubility. In this case, halite dissolution may occur in the walls of fluid inclusions, and Cl
486 enrichment and increase of Cl/Br ratios are expected in the residual brines. Cl concentrations
487 and Cl/Br shifts in the residual brines can be roughly modelled using halite solubility in the
488 H_2O-NaCl system (Bodnar, 1994) and assuming a negligible Br content of halite. Fig. 6
489 shows that Cl concentrations could shift from 150,000 ppm (halite solubility at 25°C) to

190,000 ppm (200°C). If the evaporated seawater was trapped at the final stage of halite precipitation, Cl/Br ratios would shift from 235 (25°C) to 280 (200°C).

The deepest potential evaporitic formation that could have enclosed such brines was located at least 1,5 km above the unconformity (Carswell Formation). Assuming a past thickness of 5 km for the sedimentary pile, and a geothermal gradient of 30-35°C/km, a maximum temperature of ~130°C for the evaporitic formation before expulsion of enclosed brines can reasonably be assumed.

The temperatures of 100-150°C necessary to account for significant Cl concentration and Cl/Br ratio shifts from the seawater evaporation trend are in the lower range of temperatures estimated for the brines that have circulated at the base of the Athabasca sandstones and in the basement (Derome et al., 2005; Richard, 2009). Assuming that evaporated seawater was initially trapped within evaporites from the Carswell Formation, re-equilibration with halite during burial at 100-150°C could have significantly affected the Cl content, Cl/Br ratios and $\delta^{37}Cl$ values, before their expulsion towards basal sandstones.

6.2.3. Dilution of brines

NaCl-rich brine inclusions have salinity predominantly ranging from ~20 to ~30 eq. wt% NaCl which corresponds to Cl concentrations ranging from ~120,000 to ~180,000 ppm (Table 1). The Cl concentration of halite-saturated seawater is close to 150,000 ppm (Fontes and Matray, 1993) and thus a significant amount of NaCl-rich brine inclusions have a Cl content lower than that of halite-saturated seawater.

Thus, the evaporated seawater may have undergone some dilution during percolation towards the base of the Athabasca sandstones, which can be expected when evaporated seawater percolates through the sedimentary pile and encounters connate and/or formation

515 waters. From the mixing scenario between halite-to-sylvite-saturated evaporated seawater
516 (Cl/Br ~100) and meteoric water or seawater (Cl/Br ~650) (Fig. 5), this dilution would not
517 affect Cl/Br ratios unless the evaporated seawater was mixed with more than 80% of diluting
518 fluid. From Fig. 5, we consider that a maximum of 30% of diluting fluid was added to
519 evaporated seawater to account for the lowest salinities observed in NaCl-rich brine
520 inclusions.
521
522 *6.2.4. Cl leaching in the Athabasca Basement*
523
524 Biotites and amphiboles are the main Cl-bearing minerals in igneous and metamorphic
525 rocks and can contain from several hundreds to thousands of ppm of Cl (Kamineni, 1984).
526 Kamineni (1984) has shown that amphibole and biotite breakdown by 100-300°C
527 hydrothermal fluids in the East Bull Lake anorthosite-gabbro complex, was followed by
528 precipitation of Cl-free minerals including various clay minerals. This may explain part of the
529 Cl content of the present-day interstitial waters. Richard (2000) has shown that shield brines
530 could contain up to 0.5 molal of Cl inherited from a Cl-OH exchange reaction with biotites.
531 In the Athabasca Basement, plutonic rocks together with pelitic gneisses are the main
532 biotite-bearing rocks. Table 3 shows that in porphyry granites and pegmatites from the
533 Athabasca Basement, fresh biotites have an average Cl concentration of ~3,800 ppm. In their
534 altered counterparts, illite and sudoite replace biotites and have an average Cl content of 280
535 and 360 ppm respectively. At the whole rock scale, Cl loss from biotites during alteration of
536 Athabasca Basement rocks by the studied brines is illustrated in Fig. 7. With increasing
537 alteration, as shown by increasing L.O.I., the Cl content of fresh rock decreases rapidly by
538 about one order of magnitude. Thus, Athabasca Basement rocks may have lost up to 90% of

their initial Cl during alteration and could be a potential additional Cl source for the studied brines (Fig. 4).

In this case, the Cl/Br ratios would shift depending of the Cl/Br ratios of the biotites and amphiboles which are highly variable (Fuge, 1974) and unknown for the Athabasca Basement rocks, as are the $\delta^{37}Cl$ compositions. Ranges of published $\delta^{37}Cl$ of various fluids, rocks and minerals of interest for the interpretation of $\delta^{37}Cl$ values of Athabasca brines are shown in Fig. 8. Considering published $\delta^{37}Cl$ values of biotites and amphiboles, a shift towards positive $\delta^{37}Cl$ values is expected if leaching of basement-derived Cl occurs. The amount of basement-derived Cl in the studied brines will depend on the fluid rock ratios which could have been highly variable on a local scale. Assuming localized low fluid-rock ratios in Cl-rich basement rocks (i.e. pelites, amphibolites), we can reasonably assume that some fluids may locally contain a significant proportion of basement-derived Cl (Fig. 4).

6.2.5. Water uptake from brines to alteration minerals

Surface-derived fluids may undergo significant salinity increase during percolation in basement rocks during retrograde hydration reactions (Gleeson et al., 2003). In the Athabasca Basement, altered rocks have L.O.I. up to 10% while fresh rocks have L.O.I. up to 2% (Fig. 7). Mercadier et al., (2010) have shown that the most intensively altered basement rocks at P-Patch, were associated with the most saline brines. As for Cl leaching within basement rocks, water uptake from brines to alteration minerals could have partly enhanced the chlorinity depending on the fluid-rock ratios.

562 **6.3. The missing link to the source of chlorine**

563

564 The formation of uranium ore-forming brines in the Athabasca Basin has required
565 large-scale evaporitic processes and the deposition of large amounts of evaporites. In the
566 preserved part of the basin, there is no evidence for massive evaporites (Ramaekers et al.,
567 2007). Hendry and Weathley (1985) noted that periodic evaporation left gypsum in the
568 Carswell Formation and evidenced solution-collapse breccias following dissolution of
569 evaporites at depth. Sediments of the Carswell Formation are only preserved around the
570 Carswell structure (Fig. 1) and the original extent of the Carswell Formation was probably
571 much larger (Hendry and Weathley, 1985). Thus, before erosion, the entire Carswell
572 Formation potentially hosted a large amount of evaporite minerals. Note that the present-day
573 thickness of the preserved sedimentary pile is ~1,5 km (Ramaekers et al., 2007) and that fluid
574 inclusion data yielded a past thickness of 4-6 km (Pagel 1975; Derome et al., 2005). Thus,
575 most of the sediments potentially containing evaporites have been removed by erosion and/or
576 dissolution. The relationship between high salinity brines and evaporite deposits is much
577 more evident in the Kombolgie sub-Basin (Australia). This hosts similar U deposits to those
578 of the Athabasca Basin and evaporites are widely described in area (Walker et al., 1977;
579 Warren, 2000, Rawlings, 1999).

580 If the paleolatitude was known during sedimentation in the Athabasca Basin, then the
581 possibility of the existence of evaporitic basins might become clearer. However, the timing of
582 sedimentation in the Athabasca Basin is poorly constrained. The onset of sedimentation is
583 thought to have occurred at ~1.75 Ga (Ramaekers et al., 2007), but the age of the end of
584 sedimentation is unknown. The age of the Carswell Formation could be considered as a
585 minimum age for possible seawater evaporation in the Athabasca Basin. Unfortunately, its
586 age is also unknown. Re-Os geochronology on organic–rich black shales of the underlying

Douglas Formation yielded depositional ages of 1541 ± 13 Ma (Creaser and Stasiuk, 2007). Thus, in order to evaluate the possibility of evaporitic environments during formation of the Athabasca Basin, the paleolatitudes of Northern Saskatchewan must be considered between 1.5 Ga (approximate age for the Carswell Formation) and 1.3 Ga (minimum age for primary uranium mineralizations) (Cummings and Krstic, 1992; Fayek et al., 2002; Alexandre et al., 2009). Paleomagnetic reconstructions suggest that Northern Saskatchewan was located within 30° of the equator between 1.5 Ga and 1.3 Ga and possibly within 5° during periods (Kotzer et al., 1992; Buchan et al., 2000; Meert et al., 2002; Pesonen et al., 2003; Zhao et al., 2004). Thus, low latitudes of the Northern Saskatchewan area during sedimentation of the Athabasca Basin could have favoured evaporitic environments and the production of halite deposits and evaporated seawater.

6.4. A model for the genesis and migration of uranium ore-forming brines

Fig. 9 shows a model that summarizes the evolution of Cl concentrations, Cl/Br ratios and $\delta^{37}Cl$ values of the different fluid reservoirs and interaction between them, leading to the measured values in the NaCl-rich and $CaCl_2$-rich brines. Although the evaporation of seawater appears to be the dominant process at the origin of the high-chlorinity brines, the analyzed ore-forming brines have undergone minor modification of their chlorinity, Cl/Br ratios and $\delta^{37}Cl$ values through interaction with meteoric water and/or seawater, evaporites, and basement rocks. One of the main uncertainties concerns the storage of evaporated seawater within the evaporitic formation or the direct downward percolation of evaporated seawater from the surface. At this stage, neither of the two hypotheses can be reasonably favored, both scenarios being able to generate large amounts of brines with compatible geochemical signatures. Meteoric water and/or seawater are involved in the generation of

612 halite-dissolution brine and dilution of the mixture between evaporated seawater and the
613 halite-dissolution brines ("parent brine" in Fig. 9). The slight dilution of this parent brine is
614 expected during its percolation towards the base of the basin when encountering connate
615 and/or formation waters. Thermally-driven free convection may have been the main force
616 driving brines towards the basal Athabasca sandstones and basement rocks (Raffensperger
617 and Garven, 1995b; Boiron et al., 2010).
618
619 **7. CONCLUSION**
620
621 The chlorinity, Cl/Br ratio and $\delta^{37}Cl$ signature of the Athabasca brines linked to the
622 formation of unconformity-related uranium deposits indicate a complex history of acquisition
623 of high salinities and allow us to draw the following conclusions:
624 (1) High chlorinities were acquired by surface evaporation of seawater favoured by
625 low-latitudes of the Northern Saskatchewan area between 1.5 and 1.2 Ga.
626 (2) The chemically distinct NaCl-rich and $CaCl_2$-rich brines have comparable Cl/Br
627 ratios and $\delta^{37}Cl$ signatures and thus share a common evaporated seawater origin.
628 (3) The chlorinity, Cl/Br ratios and $\delta^{37}Cl$ signatures of the initial evaporated seawater
629 might have been subsequently affected by: (i) mixing with halite-dissolution brines or re-
630 equilibration with host-halite at high temperature during burial; (ii) slight dilution by connate
631 and/or formation waters; (iv) leaching of chlorine in basement rocks; (iii) water uptake from
632 brines to alteration minerals.
633 This study shows that in a context of intense fluid-rock interaction and due to their
634 conservative behavior, Cl/Br ratios coupled with $\delta^{37}Cl$ signatures are powerful tools to
635 unravel the mechanisms for the acquisition of the salinity of crustal fluids.
636

ACKNOWLEDGEMENTS

The authors acknowledge CNRS and Areva NC for the financial support (BDI PhD grant for A. Richard and J. Mercadier). Areva NC and Cameco are also thanked for providing the samples and scientific collaboration. This article has benefited from fruitful discussion with Philippe Muchez, Bruce Yardley and Mark Kendrick. Environment Canada staff is warmly acknowledged for providing stable chlorine isotope analyses of fluid inclusion leachates. Ray Burgess and two anonymous reviewers are greatly thanked for their constructive remarks as well as Dimitri Sverjensky for his careful editorial handling.

REFERENCES

Alexandre P., Kyser K., Polito P. and Thomas D. (2005) Alteration mineralogy and stable isotope geochemistry of Paleoproterozoic basement-hosted unconformity-type uranium deposits in the Athabasca Basin, Canada. *Econ. Geol.* **100**, 1547-1563.

Alexandre P., Kyser K., Thomas D., Polito P. and Marlat J. (2009) Geochronology of unconformity-related uranium deposits in the Athabasca Basin, Saskatchewan, Canada and their integration in the evolution of the basin. *Miner. Deposita* **44**, 41-59.

Annesley I.R. and Madore C. (1999) Leucogranites and pegmatites of the sub-Athabasca basement, Saskatchewan: U protore? In: Stanley, C.J. et al. (eds): *Mineral Deposits: Processes to Processing*. Balkema, Rotterdam, 297-300.

Annesley I.R., Madore C. and Portella P. (2005) Geology and thermotectonic evolution of the western margin of the Trans-Hudson Orogen: Evidence from the eastern sub-Athabasca basement, Saskatchewan. *Can. J. Earth Sci.* **42**, 573-597.

661 Banks D.A. and Yardley B.W.D. (1992) Crush-leach analysis of fluid inclusions in small
662 natural and synthetic samples. *Geochim. Cosmochim. Acta* **56**, 245-248.
663 Banks D.A., Green R., Cliff R.A. and Yardley B.W.D. (2000a) Chlorine isotopes in fluid
664 inclusions: determination of the origins of salinity in magmatic fluids. *Geochim.*
665 *Cosmochim. Acta* **64**, 1785-1789.
666 Banks D.A., Guiliani G., Yardley B.W.D. and Cheilletz A. (2000b) Emerald mineralization in
667 Colombia: fluid chemistry and the role of brine mixing. *Miner. Deposita* **35**, 699-713.
668 Banks D.A., Gutzmer J., Lüders V., Beukes N.J. and Von Bezing K.L. (2003) The
669 composition of seawater in the Palaeoproterozoic. *Trans. Inst. Min. Metall., Section B:*
670 *Applied Earth Science*, **112**, B153-B154.
671 Bodnar R.J. (1994) Synthetic fluid inclusions: XII. The system H_2O-NaCl. Experimental
672 determination of the halite liquidus and isochores for a 40 wt% NaCl solution.
673 *Geochim. Cosmochim. Acta* **58**, 1053-1063.
674 Böhlke J.K. and Irwin J.J. (1992) Laser microprobe analyses of Cl, Br, I and K in fluid
675 inclusions: Implications for sources of salinity in some ancient hydrothermal fluids.
676 *Geochim. Cosmochim. Acta* **56**, 203-225.
677 Boiron M.C., Cathelineau M. and Richard A. (2010) Fluid flows and metal deposition near
678 basement / cover unconformity: Lessons and analogies from Pb-Zn-F-Ba systems for
679 the understanding of Proterozoic U deposits. *Geofluids* **10**, 270-292.
680 Boudreau A.E., Stewart M.A. and Spivack A.J. (1997) Stable Cl isotopes and origin of high-
681 Cl magmas of the Stillwater Complex, Montana. *Geology* **25**, 791-794.
682 Bray C.J., Spooner T.C. and Longstaffe F.J. (1988) Unconformity-related uranium
683 mineralization, McClean deposits, North Saskatchewan, Canada: hydrogen and
684 oxygen isotope geochemistry. *Can. Mineral.* **26**, 249-268.

685 Buchan K.L., Mertanen S., Park R.G., Pesonen L.J., Elming S.Å., Abrahamsen N. and Bylund
686 G. (2000) Comparing the drift of Laurentia and Baltica in the Proterozoic: the
687 importance of key palaeomagnetic poles. *Tectonophysics* **319**, 167-198.
688 Card C.D. (2002) New investigations of basement to the Western Athabasca Basin. *Summary*
689 *of investigations 2002*, Volume 2, Saskatchewan Geological Survey, Sask. Industry
690 Resources, Misc. Rep. 2002-4.2.
691 Card C.D., Campbell J.E. and Slimmon W.L. (2003) Basement lithologic framework and
692 structural features of the Western Athabasca Basin. *Summary of investigations 2003*,
693 Volume 2, Saskatchewan Geological Survey, Sask. Industry Resources, Misc. Rep.
694 2003-4.2, 17 p
695 Card C.D., Pana D., Portella P., Thomas D.J., Annesley I.R. (2007) Basement rocks to the
696 Athabasca Basin, Saskatchewan and Alberta, in C.W. Jefferson and G. Delaney (eds.)
697 EXTECH IV: Geology and Uranium EXploration TECHnology of the Proterozoic
698 Athabasca Basin, Saskatchewan and Alberta. *Geological Survey of Canada Bulletin*
699 **588**, 69-87.
700 Carpenter A.B., Trout M.L. and Pickett E.E. (1974) Preliminary report on the origin and
701 chemical evolution of lead- and zinc-rich brines in central Mississipi. *Econ. Geol.* **69**,
702 1191-1206.
703 Channer D.M.D., De Ronde C.E.J. and Spooner E.T.C. (1997) The Cl^--Br^--I^- composition of ~
704 3.23 Ga modified seawater: Implications for the geological evolution of ocean halide
705 chemistry. *Earth Planet. Sci. Lett.* **150**, 325-335.
706 Chi G. and Savard M.M. (1997) Sources of basinal and Mississippi Valley-type mineralising
707 brines: mixing of evaporated seawater and halite-dissolution brine. *Chem. Geol.* **143**,
708 121-125.

709 Chiaradia M., Banks D.A., Cliff R., Marschik R. and Haller A. (2006) Origin of fluids in iron
710 oxide-copper-gold deposits: Constraints from $\delta^{37}Cl$, $^{87}Sr/^{86}Sr_i$ and Cl/Br. *Mineral.*
711 *Deposita* **41**, 565-573.
712 Chiarenzelli J., Aspler L., Villeneuve M. and Lewry J. (1998) Early Proterozoic evolution of
713 the Saskatchewan craton and its allochtonous cover, Trans-Hudson orogen. *J. Geol.*
714 **106**, 247-267.
715 Creaser R.A. and Stasiuk L.D. (2007) Depositional age of the Douglas Formation, Northern
716 Saskatchewan, determined by Re-Os geochronology. In C.W. Jefferson and G.
717 Delaney (eds.) EXTECH IV: Geology and Uranium EXploration TECHnology of the
718 Proterozoic Athabasca Basin, Saskatchewan and Alberta. *Geological Survey of*
719 *Canada Bulletin* **588**, 341-346.
720 Cumming G.L. and Krstic D. (1992) The age of unconformity-related uranium mineralization
721 in the Athabasca Basin, Northern Saskatchewan. *Can. J. Earth Sc.* **29**, 1623-1639.
722 Derome D., Cuney M., Cathelineau M., Fabre C., Dubessy J., Bruneton P. and Hubert A.
723 (2003) A detailed fluid inclusion study in silicified breccias from the Kombolgie
724 sandstones (Northern Territory, Australia): inferences for the genesis of middle-
725 Proterozoic unconformity-type uranium deposits. *J. Geochem. Explor.* **80**, 259-275.
726 Derome D., Cathelineau M., Cuney M., Fabre C., Lhomme T. and Banks D.A. (2005) Mixing
727 of sodic and calcic brines and uranium deposition at McArthur River, Saskatchewan,
728 Canada: A Raman and laser-induced breakdown spectroscopic study of fluid
729 inclusions. *Econ. Geol.* **100**, 1529-1545.
730 Derome D., Cathelineau M., Fabre C., Boiron M.C., Banks D., Lhomme T. and Cuney M.
731 (2007) Paleo-fluid composition determined from individual fluid inclusions by Raman
732 and LIBS: Application to mid-proterozoic evaporitic Na-Ca brines (Alligator Rivers
733 Uranium Field, northern territories Australia). *Chem. Geol.* **237**, 240-254.

734 De Ronde C.E.J., Channer D.M.D., Faure K., Bray C.J. and Spooner E.T.C. (1997) Fluid
735 chemistry of Archean seafloor hydrothermal vents: Implications for the composition
736 of circa 3.2 Ga seawater. *Geochim. Cosmochim. Acta* **61**, 4025-4042.
737 Eastoe C.J., Guilbert J.M. and Kaufmann R.S. (1989) Preliminary evidence for fractionation
738 of stable chlorine isotopes in ore-forming hydrothermal systems. *Geology* **17**, 285-
739 288.
740 Eastoe C.J. and Guilbert J.M. (1992) Stable chlorine isotopes in hydrothermal processes.
741 *Geochim. Cosmochim. Acta* **56**, 4247-4255.
742 Eastoe C.J. and Peryt T. (1999) Stable chlorine isotope evidence for non-marine chloride in
743 Badenian evaporites, Carpathian mountain region. *Terra Nova* **11**, 118-123.
744 Eastoe C.J., Long A. and Knauth L.P. (1999) Stable chlorine isotopes in the Palo Duro Basin,
745 Texas: evidence for preservation of Permian evaporite brines. *Geochim. Cosmochim.*
746 *Acta* **63**, 1375-1382.
747 Eastoe C.J., Peryt T.M., Petrychenko O.Y. and Geisler-Cussey D. (2007) Stable chlorine
748 isotopes in Phanerozoic evaporites. *Appl. Geochem.* **22**, 575-588.
749 Eggenkamp H.G.M. and Schuiling R.D. (1995) δ^{37}Cl variations in selected minerals: a
750 possible tool for exploration. *J. Geochem. Explor.* **55**, 249-255.
751 Eggenkamp H.G.M., Kreulen R. and Koster Van Groos A.F. (1995) Chlorine stable isotope
752 fractionation in evaporites. *Geochim. Cosmochim. Acta* **59**, 5169-5175.
753 Fayek M. and Kyser T.K. (1997) Characterization of multiple fluid-flow events and rare-
754 earth-element mobility associated with formation of unconformity-type uranium
755 deposits in the Athabasca Basin, Saskatchewan. *Can. Mineral.* **35**, 627-658.
756 Fayek M., Kyser T.K. and Riciputi L.R. (2002) U and Pb isotope analysis of uranium
757 minerals by ion microprobe and the geochronology of McArthur River and Sue Zone
758 uranium deposits, Saskatchewan, Canada. *Can. Mineral.* **40**, 1553-1569.

759 Fontes J.C. and Matray J.M. (1993) Geochemistry and origin of formation brines from the
760 Paris Basin, France 1. Brines associated with Triassic salts. *Chem. Geol.* **109**, 149-
761 175.

762 Foriel J., Philippot P., Rey P., Somogyi A., Banks D.A. and Ménez B. (2004) Biological
763 control of Cl/Br and low sulfate concentration in a 3.5-Gyr-old seawater from North
764 Pole, Western Australia. *Earth Planet. Sci. Lett.* **228**, 451-463.

765 Fuge R. (1974) Chapter. 17 and 35. In Wedehpohl K.H. (ed.) *Handbook of Geochemistry*,
766 Springer, Berlin.

767 Gleeson S.A. (2003) Bulk analysis of electrolytes in fluid inclusions. In Samson I., Anderson
768 A. and Marshall D. (eds.), Fluid inclusions: Analysis and Interpretation. *Mineralogical*
769 *Association of Canada Short Course Series* **32**, 233-246.

770 Gleeson S.A., Yardley B.W.D., Boyce A.J., Fallick A.E. and Munz I.A. (2003) Infiltration of
771 basinal fluids into high-grade basement South Norway: sources and behaviour of
772 waters and brines. *Geofluids* **3**, 33-48.

773 Gleeson S.A. and Smith M.P. (2009) The sources and evolution of mineralising fluids in iron
774 oxide-copper-gold systems, Norrbotten, Sweden: Constraints from Br/Cl ratios and
775 stable Cl isotopes of fluid inclusion leachates. *Geochim. Cosmochim. Acta*. **73**, 5658-
776 5672.

777 Godon A.R., Jendrzejewski N., Eggenkamp H.G.M., Banks D.A., Ader M., Coleman M.L.
778 and Pineau F. (2004) A cross-calibration of chlorine isotopic measurements and
779 suitability of seawater as the international reference material. *Chem. Geol.* **207**, 1-12.

780 Grandia F., Canals A., Cardellach E., Banks D.A. and Perona J. (2003a) Origin of ore-
781 forming brines in sediment hosted Zn-Pb deposits of the Basque-Cantabrian Basin,
782 Northern Spain. *Econ. Geol.* **98**, 1397-1411.

783 Grandia F., Cardellach E., Canals A. and Banks D.A. (2003b) Geochemistry of the fluids
784 related to epigenetic carbonate-hosted Zn-Pb deposits in the Maestrat Basin, Eastern
785 Spain: fluid inclusion and isotope (Cl, C, O, S, Sr) evidence. *Econ. Geol.* **98**, 933-954.
786 Hanor J.S. (1994) Origin of saline fluids in sedimentary basins. In Parnell J. (ed.) Geofluids:
787 Origin, Migration and Evolution of Fluids in Sedimentary Basins. *Geol. Soc. Spec.*
788 *Publ.* **78**, 151-174.
789 Hecht L. and Cuney M. (2000) Hydrothermal alternation of monazite in the Precambrian
790 crystalline basement of the Athabasca Basin (Saskatchewan, Canada): Implications for
791 the formation of unconformity-related uranium deposits. *Mineral. Deposita* **35**, 791-
792 795.
793 Hendry H.E. and Weathley K.L. (1985) The Carswell Formation, Northern Saskatchewan:
794 Stratigraphy, sedimentology, and structure. In Lainé R., Alonso D. and Svab M. (eds.)
795 The Carswell Structure Uranium Deposits, Saskatchewan. *Geological Association of*
796 *Canada Special Paper* **29**, 87-103.
797 Hoeve J. and Sibbald T.I.I. (1978) On the genesis of the Rabbit Lake and other unconformity-
798 type uranium deposits in Northern Saskatchewan, Canada. *Econ. Geol.* **73**, 1450-1473.
799 Hoeve J. and Quirt D. (1984) Mineralization and host rock alteration in relation to clay
800 mineral diagenesis and evolution of the middle Proterozoic Athabasca basin, Northern
801 Saskatchewan, Canada. *Saskatchewan Research Council Technical Report* 187, 190 p.
802 Hoffman P.F. (1990) Subdivision of the Churchill Province and extent of the Trans-Hudson
803 Orogen. In Lewry J.F. and Stauffer M.R. (eds.) The Early Proterozoic Trans-Hudson
804 Orogen of North America. *Geological Association of Canada Special Paper* **37**, 15-
805 39.
806 Jefferson C.W., Thomas D.J., Gandhi S.S., Ramaekers P., Delaney G., Brisbin D., Cutts C.,
807 Portella P. and Olson R.A. (2007) Unconformity associated uranium deposits of the

Athabasca Basin, Saskatchewan and Alberta. In Jefferson C.W. and Delaney G. (eds.) EXTECH IV: Geology and Uranium EXploration TECHnology of the Proterozoic Athabasca Basin, Saskatchewan and Alberta. *Geological Survey of Canada Bulletin* **588,** 23-67.

Kamineni D.C. (1984) Halogen-bearing minerals in plutonic rocks: a possible source of chlorine in saline groundwater in the Canadian Shield. In Fritz P. and Frape S.K. (eds.) Saline water and gases in crystalline rocks. *Geological Association of Canada Special Paper* **33**, 69-79.

Kaufmann R., Long A., Bentley H. and Davis S. (1984a) Natural chlorine isotope variations. *Nature* **309**, 338-340.

Kaufmann R., Frape S.K., Fritz P. and Bentley H. (1984b) Chlorine stable isotope composition of Canadian Shield brines. In Fritz P. and Frape S.K. (eds.) Saline water and gases in crystalline rocks. *Geological Association of Canada Special Paper* **33**, 89-93.

Kesler S.E., Appold M.S., Martini A.M., Walter L.M., Huston T.J. and Kyle J.R. (1995) Na-Cl-Br systematics of mineralizing brines in Mississippi Valley-type deposits. *Geology* **23**, 641-644.

Koehler G. and Wassenaar L.I. (2010) The stable isotopic composition ($^{37}Cl/^{35}Cl$) of dissolved chloride in rainwater. *Appl. Geochem.* **25**, 91-96.

Komninou A. and Sverjensky D.A. (1996) Geochemical modeling on the formation of an unconformity-type uranium deposit. *Econ. Geol.* **91**, 590-606.

Kotzer T.G., Kyser T.K. and Irving E. (1992) Paleomagnetism and the evolution of fluids in the Proterozoic Athabasca Basin, Northern Saskatchewan, Canada. *Can. J. Earth Sci.* **29**, 1474-1491.

832 Kotzer T.G. and Kyser T.K. (1995) Petrogenesis of the Proterozoic Athabasca Basin,
833 Northern Saskatchewan, Canada, and its relation to diagenesis, hydrothermal uranium
834 mineralization and paleohydrogeology. *Chem. Geol.* **120**, 45-89.
835 Kyser T.K., Hiatt E., Renac C., Durocher K., Holk G. and Deckart K. (2000) Diagenetic
836 fluids in paleo- and meso-proterozoic sedimentary basins and their implications for
837 long protracted fluid histories. In Kyser K. (ed.) Fluids and basin evolution.
838 *Mineralogical Association of Canada Short Course Series* **28**, 225-262.
839 Kyser T.K and Cuney M (2008) Unconformity-related uranium deposits. In Cuney M. and
840 Kyser K. (eds.) Recent and Not-So-Recent Developments in Uranium Deposits and
841 Implications for Exploration. *Mineralogical Association of Canada Short Course*
842 *Series* **39**, 161-219.
843 Liu W.G., Xiao Y.K., Wang Q.Z., Qi H.P., Wang Y.H., Zhou Y.M. Shirodkar P.V. (1997)
844 Chlorine isotopic geochemistry of salt lakes in the Qaidam Basin, China. *Chem. Geol.*
845 **136**, 271-279.
846 Magenheim A.J., Spivack A.J., Michael P.J. and Gieskes J.M. (1995) Chlorine stable isotope
847 composition of the oceanic crust: Implications for Earth's distribution of chlorine.
848 *Earth Plan. Sci. Lett.* **131**, 427-432.
849 Madore C., Annesley I.R. and Wheatley K. (2000) Petrogenesis, age and uranium fertility of
850 peraluminous leucogranites and pegmatites of the McClean Lake / Sue and Key Lake /
851 P-Patch deposits area, Saskatchewan. *Geocanada 2000. The Millennium Geoscience*
852 *Summit,* Calgary, Program with Abstracts, 1041-1044.
853 Markl G., Musashi M. and Bucher K. (1997) Chlorine stable isotope composition of
854 granulites from Lofoten, Norway: Implications for the Cl isotopic composition and for
855 the source of Cl enrichment in the lower crust. *Earth Plan. Sci. Lett.* **150**, 95-102.

McGowan R.R., Roberts S. and Boyce A.J. (2006) Origin of the Nchanga copper-cobalt deposits of the Zambian Copperbelt. *Mineral. Deposita* **40**, 617-638.

Meert J.G. (2002) Paleomagnetic Evidence for a Paleo-Mesoproterozoic Supercontinent Columbia. *Gondwana Res.* **5**, 207-215.

Mercadier J. (2008) Conditions de genèse des gisements d'uranium associés aux discordances protérozoïques et localisés dans les socles. Exemple du socle du bassin d'Athabasca (Saskatchewan, Canada). Unpublished PhD Thesis, Institut National Polytechnique de Lorraine, Nancy, France, 362 p.

Mercadier J., Richard A., Boiron M.C., Cathelineau M. and Cuney M. (2010) Brine migration in the basement rocks of the Athabasca Basin through microfracture networks (P-Patch U deposit, Canada). *Lithos* **115**, 121-136.

Mercadier J., Cuney M., Cathelineau M. and Lacorde M. (2011) U redox fronts and kaolinisation in basement-hosted unconformity-related U ores of the Athabasca Basin (Canada): late U remobilisation by meteoric fluids. *Mineral. Deposita* **46**, 105-135.

Möller P., Woith H., Dulski P., Lüders V., Erzinger J., Kämpf H., Pekdeger A., Hansen B., Lodemann M. and Banks D.A. (2005) Main and trace elements in KTB-VB fluid: composition and hints to its origin. *Geofluids* **5**, 28-41.

Muchez P., Heijlen W., Banks D.A., Blundell D., Boni M. and Grandia F. (2005) Extensional tectonics and the timing and formation of basin-hosted deposits in Europe. *Ore Geol. Rev.* **27**, 241-267.

Musashi M., Markl G. and Kreulen R. (1998) Stable chlorine-isotope analysis of rock samples: New aspects of chlorine extraction. *Anal. Chim. Acta* **362**, 261-269.

Nahnybida T., Gleeson S.A., Rusk B.G. and Wassenaar L.I. (2009) Cl/Br ratios and stable chlorine isotope analysis of magmatic-hydrothermal fluid inclusions from Butte, Montana and Bingham Canyon, Utah. *Mineral. Deposita* **44**, 838-848.

881 Pagel M. (1975) Détermination des conditions physico-chimiques de la silicification
882 diagénétique des grès Athabasca (Canada) au moyen des inclusions fluides. *Comptes*
883 *Rendus de l'Académie des Sciences de Paris* **280(D)**, 2301-2304.
884 Pagel M. and Jaffrezic H. (1977) Analyses chimiques des saumures des inclusions du quartz
885 et de la dolomite du gisement d'uranium de Rabbit Lake (Canada). Aspect
886 méthodologique et importance génétique. *Comptes Rendus de l'Académie des*
887 *Sciences de Paris* **284(D)**, 113-116.
888 Pagel M., Poty B. and Sheppard S.M.F. (1980) Contribution to some Saskatchewan uranium
889 deposits mainly from fluid inclusion and isotopic data. In IAEA (ed.) *International*
890 *Uranium Symposium on the Pine Creek Geosyncline*, Vienna, 639-654.
891 Pagel M., Wheatley K. and Ey F. (1985) The Origin of the Carswell circular structure. A
892 summary of data for geological interpretation of its formation. In Lainé R, Alonso D
893 and Svab M. (eds.) The Carswell Structure Uranium Deposits Saskatchewan.
894 *Geological Association of Canada Special Paper* **29**, 213-223.
895 Pesonen L.J., Elming S.Å., Mertanen S., Pisarevsky S., D'Agrella-Filho M.S., Meert J.G.,
896 Schmidt P.W., Abrahamsen N. and Bylund G. (2003) Palaeomagnetic configuration of
897 continents during the Proterozoic. *Tectonophysics* **375**, 289-324.
898 Polito P.A., Kyser T.K., Marlatt J., Alexandre P., Bajwah Z. and Drever G. (2004)
899 Significance of alteration assemblages for the origin and evolution of the Proterozoic
900 Nabarlek unconformity-related uranium deposit, Northern Territory, Australia. *Econ.*
901 *Geol.* **99**, 113-139.
902 Polito P.A., Kyser T.K., Thomas D., Marlatt J. Drever G. (2005) Re-evaluation of the
903 petrogenesis of the Proterozoic Jabiluka unconformity-related uranium deposit,
904 Northern Territory, Australia. *Mineral. Deposita.* **40**, 257-288.

905 Quirt D. (2003) Athabasca unconformity-type uranium deposits: one type of deposit with
906 many variations. *Proceedings of International Conference Uranium Geochemistry*
907 *2003,* Nancy, France, 309-312.
908 Raffensperger, J.P. and Garven, G. (1995a) The formation of unconformity-type uranium ore
909 deposits 2. Coupled hydrochemical modeling. *Am. J. Sci.* **295**, 639-696.
910 Raffensperger J.P. and Garven G. (1995b) The formation of unconformity-type uranium ore
911 deposits 1. Coupled groundwater flow and heat transport modeling. *Am. J. Sci.* **295**,
912 581-636.
913 Ramaekers P., Jefferson C.W., Yeo G.M., Collier B., Long D.G., Catuneanu O., Bernier S.,
914 Kupsch B., Post R., Drever G., McHardy S., Jircka D., Cutts C. and Wheatley K.
915 (2007) Revised geological map and stratigraphy of the Athabasca Group,
916 Saskatchewan and Alberta. In Jefferson C.W. and Delaney G. (eds.) EXTECH IV:
917 Geology and Exploration Technology of the Proterozoic Athabasca basin,
918 Saskatchewan and Alberta. *Geological Survey of Canada Bulletin* **588**, 155-578.
919 Rawlings D.J. (1999) Stratigraphic resolution of a multiphase intracratonic basin system: the
920 McArthur Basin, Northern Australia. *Aust. J. Earth Sci.* **46**, 703–723.
921 Richard L. (2000) Sur l'origine des ions chlorure dans les eaux salines des massifs granitiques
922 (A dual origin for the chloride ions of saline waters from crystalline rocks). *Comptes*
923 *Rendus de l'Académie des Sciences de Paris* **331**, 783-788.
924 Richard A. (2009) Brine migration at the basement / sedimentary cover unconformity and
925 formation of Proterozoic uranium mineralizations (Athabasca Basin, Canada)
926 Unpublished PhD Thesis, Institut National Polytechnique de Lorraine, Nancy, France,
927 239p.
928 Richard A., Pettke T., Cathelineau M., Boiron M.C., Mercadier J., Cuney M. and Derome D.
929 (2010) Brine-rock interaction in the Athabasca basement (McArthur River U deposit,

930 Canada): consequences for fluid chemistry and uranium uptake. *Terra Nova* **22**, 303-
931 308.
932 Risacher F., Alonso H. and Salazar C. (2003) The origin of brines and salts in Chilean salars:
933 a hydrochemical review. *Earth Sci. Rev.* **63**, 249-293.
934 Risacher F., Fritz B. and Alonso H. (2006) Non-conservative behavior of bromide in surface
935 waters and brines of Central Andes: A release into the atmosphere? *Geochim.*
936 *Cosmochim. Acta* **70**, 2143-2152.
937 Sie P.M.J. and Frape S.K. (2002) Evaluation of the groundwaters from the Stripa mine using
938 stable chlorine isotopes. *Chem. Geol.* **182**, 565-582.
939 Stewart M.A. and Spivack A.J. (2004) The stable-chlorine isotope compositions of natural
940 and anthropogenic materials. *Rev. Mineral. Geochem.* **55**, 231-254.
941 Stotler R.L., Frape S.K. and Shouakar-Stash O. (2010) An Isotopic Survey of δ^{81}Br and δ^{37}Cl
942 of Dissolved Halides in the Canadian and Fennoscandian Shields. *Chem. Geol.* **274**,
943 38-55.
944 Walker R.N., Muir M.D., Diver W.L., Williams N. and Wilkins N. (1977) Evidence of major
945 sulphate evaporite deposits in the Proterozoic McArthur Group, Northern Territory,
946 Australia. *Nature* **265**, 526-529.
947 Warren J.K. (2000) Evaporites, brines and base metals: Low-temperature ore emplacement
948 controlled by evaporite diagenesis. *Aust. J. Earth Sci.* **47**, 179-208.
949 Warren J.K. (2010) Evaporites through time: Tectonic, climatic and eustatic controls in
950 marine and nonmarine deposits. *Earth Sci. Rev.* **98**, 217-268.
951 Wassenaar L.I. and Koehler G. (2004) On-line technique for the determination of the δ^{37}Cl of
952 inorganic and total organic Cl in environmental samples. *Anal. Chem.* **76**, 6384-6388.

953 Wilde A.R., Mernagh T.P., Bloom M.S. and Hoffmann C.F. (1989) Fluid inclusion evidence
954 on the origin of some Australian unconformity-related uranium deposits. *Econ. Geol.*
955 **84**, 1627-1642.
956 Wilson M.R. and Kyser T.K. (1987) Stable isotope geochemistry of alteration associated with
957 the Key Lake uranium deposit, Canada. *Econ. Geol.* **82**, 1540-1557.
958 Willmore C.C., Boudreau A.E., Spivack A. and Kruger F.J. (2002) Halogens of Bushveld
959 Complex, South Africa: δ^{37}Cl and Cl/F evidence for hydration melting of the source
960 region in a back-arc setting. *Chem. Geol.* **182**, 503-511.
961 Worden R.H. (1996) Controls on halogen concentrations in sedimentary formation waters.
962 *Mineral. Mag.* **60**, 259-274.
963 Yardley B.W.D. (2005) Metal concentrations in crustal fluids and their relationship to ore
964 formation. *Econ. Geol.* **100**, 613-632.
965 Ypma P.J.M. and Fuzikawa K. (1980) Fluid inclusion and stable isotope studies of the
966 Nabarlek and Jabiluka uranium deposits, Northern Territory, Australia. In IAEA (ed.)
967 *International Uranium Symposium on the Pine Creek Geosyncline*, Vienna, 375-395.
968 Zhao G., Sun M., Wilde S.A. and Li S. (2004) A Paleo-Mesoproterozoic supercontinent:
969 Assembly, growth and breakup. *Earth Sci. Rev.* **67**, 91-123.
970
971

FIGURE CAPTIONS

FIGURE 1: Simplified geological map of the Athabasca Basin and Basement, Canada, modified from Jefferson et al., (2007). Small circles indicate main uranium deposits. Large circles indicate uranium deposits studied in this work. Basement domains are individualized by different shades of grey. TMZ: Thelon magmatic zone; WMTZ: Wollaston Mudjatik transition zone; VRSZ: Virgin River shear zone; BLSZ: Black Lake shear zone.

FIGURE 2: Example of quartz and carbonate veins, hosting fluid inclusions studied in this work. (A) Dravite + quartz vein cross-cutting graphite-rich pelitic gneiss (sample H3042-1, Eagle Point). (B) Quartz + dolomite vein cross-cutting chloritized gneiss (sample P48-3, P-Patch). (C) Typical primary liquid-vapor fluid inclusion in quartz. (D) Typical primary liquid-vapor-halite fluid inclusion in quartz. Liq.: liquid phase; Vap.: vapor phase; Hal.: halite crystal.

FIGURE 3: Cl/Br vs. Cl concentration relationships in the Athabasca brines. Seawater was first evaporated up to epsomite or sylvite saturation. The upward trend indicates mixing with a halite-dissolution brine. Error bars on data points are not shown for better visibility (see 4.1. for statements of analytical errors). Seawater evaporation trend after Fontes and Matray (1993). SW: seawater. Minerals precipitating during evaporation of seawater: G: gypsum; H: halite (H_0: onset of halite precipitation; H_3:

997 end of halite precipitation); E: epsomite; S: sylvite; C: carnallite; B: bischofite; T:
998 tachyhydrite.
999
1000 FIGURE 4: $\delta^{37}Cl$ vs. Cl/Br relationships in the Athabasca brines. Seawater was first
1001 evaporated up to epsomite or sylvite saturation. Data points that do not lie close to the
1002 seawater evaporation trends indicate possible secondary Cl enrichment. Upward trend
1003 indicates possible mixing with halite-dissolution brine or re-equilibration with host
1004 halite during burial. Rightward trend indicates Cl leaching from biotites or amphiboles
1005 within basement rocks. Field for evaporated seawater after Fontes and Matray (1993),
1006 Eastoe et al., (1999) and Eggenkamp et al., (1995). SW: seawater.
1007
1008 FIGURE 5: Cl/Br vs. Cl concentration relationships after mixing scenarios between
1009 evaporated seawater at halite to carnallite saturation and halite-dissolution brine (in
1010 equilibrium with halite at 100°C, see 6.2.1. for explanations) or meteoric water or
1011 seawater. Weight fractions of fluid in the mixture are indicated along linear mixing
1012 curves. Chlorinity ranges for NaCl-rich and $CaCl_2$-rich brines are indicated. The
1013 lowest chlorinity values for the NaCl-rich brines along with relatively large chlorinity
1014 ranges for both brines may indicate partial dilution of brines in a maximum of 30% of
1015 meteoric water and/or seawater. This dilution is expected when brines encounter
1016 connate and/or formation waters during their migration through the sedimentary pile.
1017 Seawater evaporation trend after Fontes and Matray (1993). [Cl]: Cl concentration;
1018 SW: seawater; MW: meteoric water. Minerals precipitating during evaporation of
1019 seawater: G: gypsum; H: halite (H_0: onset of halite precipitation; H_3: end of halite
1020 precipitation); E: epsomite; S: sylvite; C: carnallite; B: bischofite; T: tachyhydrite.
1021

FIGURE 6: Cl/Br vs. Cl concentration relationships after scenario for re-equilibration between evaporated seawater and host halite during burial at 100, 150 and 200°C. Cl/Br ratios and Cl concentration of brines in equilibrium with host halite between 100 and 200°C are calculated using halite solubility in the H_2O-NaCl system (Bodnar, 1994) and assuming a negligible Br content of halite. Significant shifts of Cl/Br ratios and Cl concentration from the seawater evaporation trend are expected after these scenarios, and could account for part of the dispersion of the data. Seawater evaporation trend after Fontes and Matray (1993). SW: seawater. Minerals precipitating during evaporation of seawater: G: gypsum; H: halite (H_0: onset of halite precipitation; H_3: end of halite precipitation); E: epsomite; S: sylvite; C: carnallite; B: bischofite; T: tachyhydrite.

FIGURE 7: Loss on ignition (L.O.I.) vs. Cl content in fresh and altered porphyry granites and pegmatites of the Athabasca Basement. Increasing L.O.I. indicates increasing degree of alteration. The Cl content of biotites and alteration minerals (illite and sudoite) from Eagle Point porphyry granites are also shown. The Athabasca Basement rocks may have lost up to 90% of their initial Cl during alteration by the studied brines. Leaching of basement-derived Cl could be responsible for part of the secondary Cl enrichment of the initial evaporated seawater.

FIGURE 8: Ranges of published δ^{37}Cl values of various fluids, rocks and minerals of interest for interpretation of δ^{37}Cl values of Athabasca brines. Numbers in parentheses indicate references as follows: (1) Kaufmann et al., (1984a); (2) Godon et al., (2004); (3) Eggenkamp et al., (1995); (4) Eastoe et al., (1999); (5) Eastoe et al., (2007); (6) Koehler & Wassenaar (2010); (7) Liu et al., (1997); (8) Stewart and Spivak (2004) and

1047 references therein; (9) Eastoe et al., (1989); (10) Eastoe and Guilbert (1992); (11)
1048 Grandia et al., (2003b); (12) Möller et al., (2005); (13) Kaufmann et al., (1984b); (14)
1049 Sie & Frape (2002); (15) Stotler et al., (2010); (16) Musashi et al., (1998); (17) Marlk
1050 et al., (2007); (18) Eggenkamp & Schuiling (1995); (19) Magenheim et al., (1995);
1051 (20) Boudreau et al., (1997); (21) Willmore et al., (2002). KTB: German Continental
1052 Drilling Program. MVT: Mississippi Valley Type Pb-Zn deposits.
1053
1054 FIGURE 9: Conceptual model for the genesis of high-chlorinity brines in the Athabasca Basin
1055 and Basement. Fluid reservoirs and their Cl concentration ([Cl]), Cl/Br ratios and
1056 $\delta^{37}Cl$ values are shown in boxes. Processes involved in the modification of Cl
1057 concentration, Cl/Br ratios and $\delta^{37}Cl$ values are bolded and set in italics when their
1058 influence is only inferred or minor. Evaporated seawater is the dominant source of
1059 salinity for both NaCl-rich and $CaCl_2$-rich brines involved in the uranium mineralizing
1060 events.
1061
1062
1063
1064

1065

1066

1067

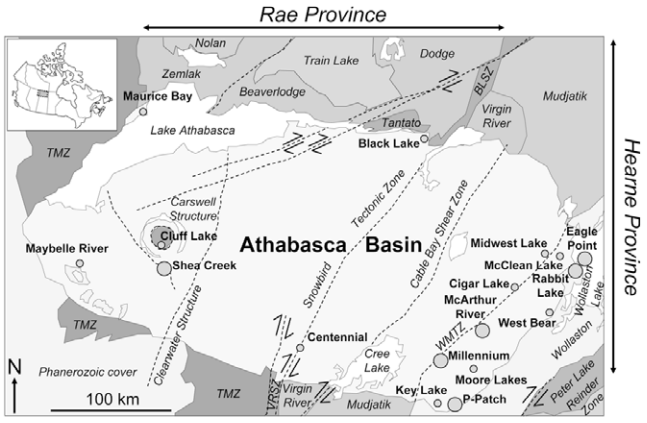

1068

1069

1070

1071

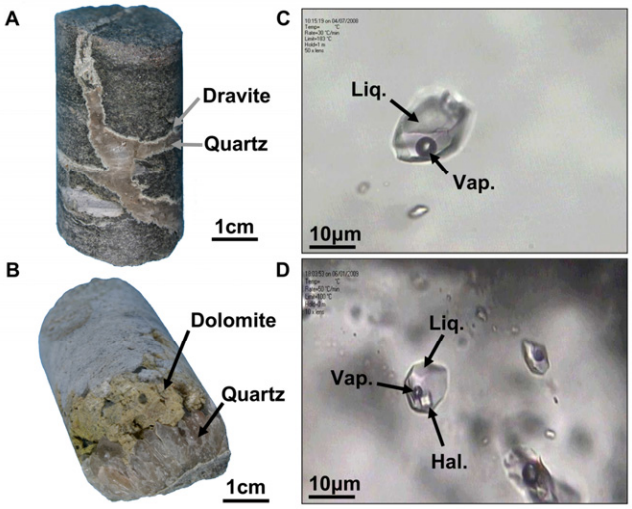

1072

1073

1074

1075

1076

1077

1078

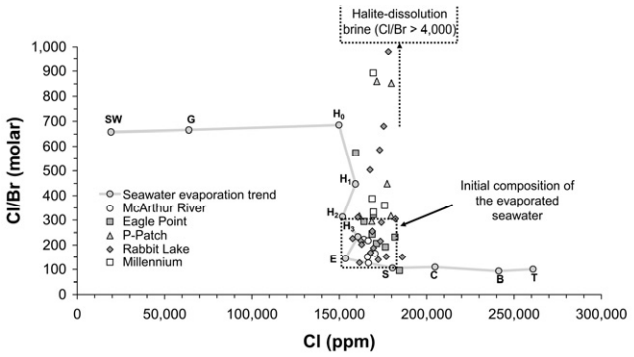

1079

1080

1081

1082

1083

1084

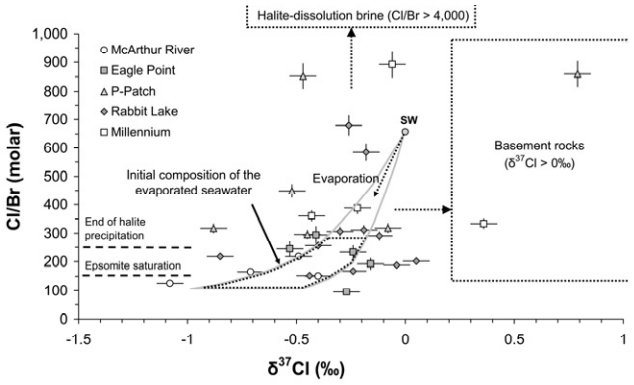

1085

1086

1087

1088

1089

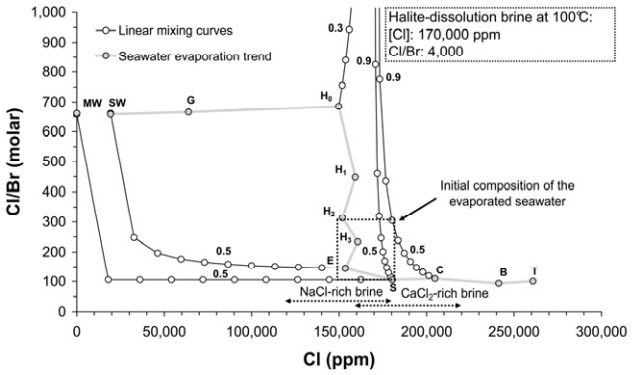

1090

1091

1092

1093

1094

1095

1096

1097

1098

1099

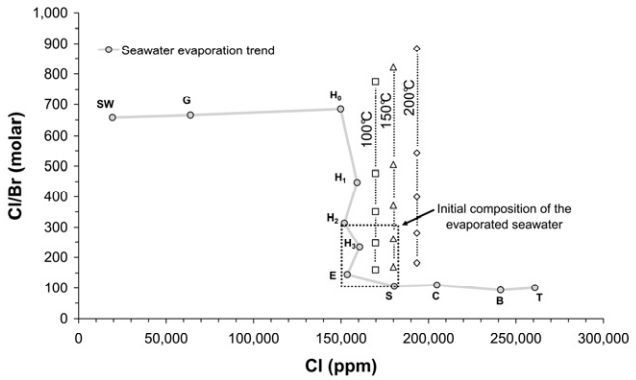

1100

1101

1102

1103

1104

1105

1106

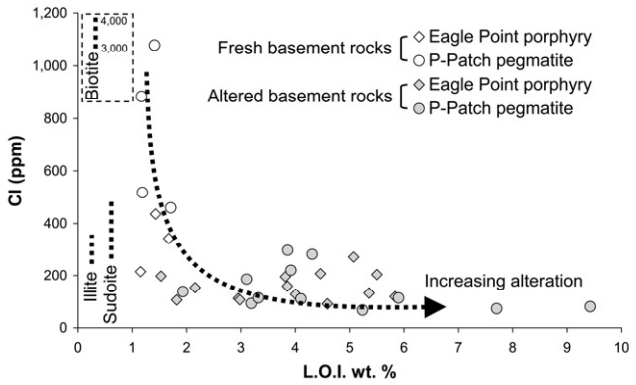

1107

1108

1109

1110

1111

1112

1113

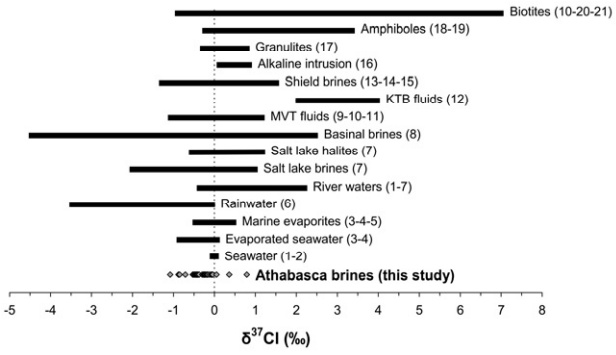

1114

1115

1116

1117

1118

1119

1120

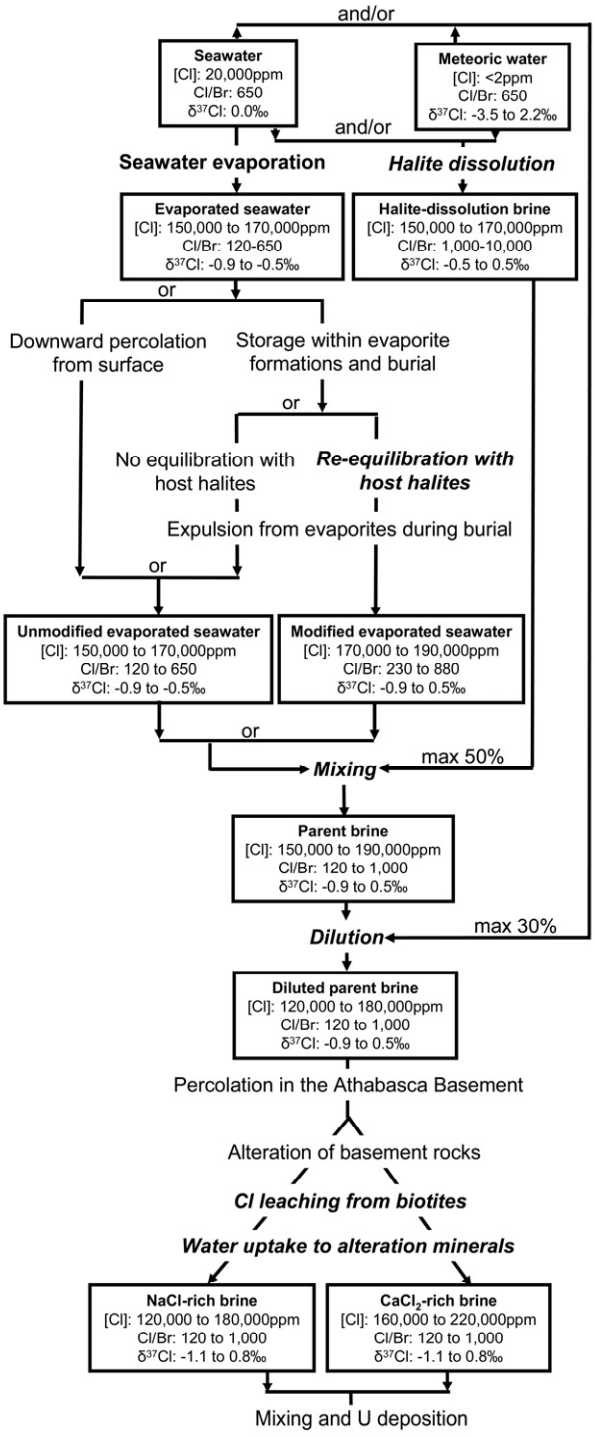

1121

TABLE CAPTIONS

TABLE 1: Summary of microthermometric characteristics of fluid inclusions, after Derome et al., (2005) and Richard (2009). All fluid inclusion types (FI type) were found in comparable amounts in the five studied deposits. Fluid inclusion types are analogous to those defined by Derome et al., (2005) for fluid inclusions from the McArthur River deposit (see text for explanation). Salinity: in weight % equivalent NaCl. Te: eutectic melting; Tm ice: ice melting; Tm hyd: hydrohalite melting; Ts NaCl: halite dissolution; Th: total homogenization (all inclusions homogenize to the liquid phase). Lw' and Lwh' inclusions frequently fail to nucleate any ice upon cooling. Modes for temperatures of phase changes and salinities are shown in parentheses.

TABLE 2: Cl/Br and $\delta^{37}Cl$ data for fluid inclusion leachates. Only fluid inclusion leachates containing more than 0.1 mg of Cl were analyzed for ^{35}Cl and ^{37}Cl. n.d.: no data; b.d.: below detection limit; * indicates that inclusions were too small to allow proper microthermometric characterization (average salinity were adjusted to the average observed salinities in other samples); FI: fluid inclusions; *N*: number fluid inclusions analyzed by microthermometry; Av.: average; U/C: unconformity. Mineral abbreviations: Qtz: quartz; Dol; dolomite; Hem: hematite; Drv: dravite; Chl: chlorite; Sst: sandstones; Pegm: pegmatoid.

TABLE 3: Cl content and loss on ignition (L.O.I) of Athabasca Basement rocks (porphyry granite, pegmatite) and minerals (biotite, illite, sudoite). *N:* number of analyses.

Fluid type	FI type	Te (°C)	Tm ice (°C)	Tm hyd (°C)	Ts NaCl (°C)	Th (°C)	Salinity
NaCl-rich brine	Lw1	-75 to -35 (-55)	-30.0 to -15.0 (-25)			60 to 193 (125)	13.2 to 30.8 (26)
	Lw2	-75 to -55 (-60)	-39.0 to -21.0 (-25)	-25.3 to 21.9 (-10)		61 to 197 (135)	23.3 to 32.6 (26)
	Lwh	-75 to -40 (-60)	-42.8 to -22.8 (-30)	-8.0 to 21.0 (-5)	81 to 208 (140)	84 to 188 (135)	28.6 to 47.1 (35)
$CaCl_2$-rich brine	Lw'	-80 to -55 (-70)	-58.0 to -30.0 (-42)			56 to 93 (115)	26.4 to 42.7 (35)
	Lwh'	-75 to -55 (-70)	-58.3 to -30.8 (-40)		99 to 265 (200)	63 to 186 (110)	27.3 to 53.8 (35)

TABLE 1

Sample	Description	Depth below U/C (m)	FI frequency (%) NaCl-rich brine	FI frequency (%) $CaCl_2$-rich brine	*N*	Av. salinity wt% eq. NaCl	Cl (ppm)	Br (ppm)	F (ppm)	SO_4 (ppm)	Cl/Br (molar)	$\delta^{37}Cl$ (‰)
Eagle Point deposit - Quartz veins												
H3042-1	Qtz+drv vein in graphite-rich gneiss	263.5	25	75	29	30.3	182,000	1,760	b.d.	b.d.	233	-0.24
ES287-8	Qtz vein in bleached pelitic gneiss	253.2	75	25	25	28.2	170,000	1,180	b.d.	b.d.	323	n.d.
ES287-10	Qtz vein in bleached pelitic gneiss	259.0	100	0	23	28.5	171,000	1,870	b.d.	b.d.	207	n.d.
EPE44-17	Qtz vein in fresh porphyry granite	131.2	55	45	29	28.2	169,000	1,560	b.d.	696	244	-0.53
DDH2306-2	Qtz vein in illitized gneiss	135.3	35	65	11	27.6	159,000	626	7,430	b.d.	573	n.d.
DDH2306-1	Qtz+sulfides vein in illitized pegm	130.0	25	75	26	29.9	176,000	2,060	177	2,480	193	-0.16
Eagle Point deposit - Dolomite veins												
H1935-8	Dol+hem vein in biotite gneiss	177.9	80	20	10	31.2	184,000	4,350	b.d.	373	95	-0.27
ES287-1	Qtz+dol vein in fresh pelitic gneiss	39.9	*	*	*	28.0	164,000	1,260	b.d.	4,420	294	-0.41
McArthur River deposit - Quartz veins												
MAC5Qz	Qtz vein surrounding U ore	25	70	30	34	28.7	170,000	2,330	b.d.	1,370	165	-0.71
MAC54Qz	Qtz+sulfides in chlorite-rich breccia	50.0	100	0	54	27.5	164,000	1,650	b.d.	1,020	224	n.d.
MAC8Qz	Qtz+sulfides vein in silicified sst	n.d.	40	60	45	28.0	167,000	1,720	b.d.	1,590	218	-0.49
MAC13Qz	Qtz+drv breccia in silicified sst	n.d.	40	60	45	28.0	166,000	2,480	b.d.	1,120	151	-0.4
McArthur River deposit - Dolomite veins												
MAC5Carb	Dol vein surrounding U ore	25.0	*	*	*	28.0	167,000	2,990	117	b.d.	126	-1.08
P-Patch deposit - Quartz veins												
P48-2	Qtz vein in chloritized gneiss	39	55	45	27	29.9	180,000	1,270	763	b.d.	318	-0.08
P48-3Qz	Qtz+dol vein in chloritized gneiss	40	45	55	20	29.4	177,000	891	b.d.	b.d.	449	-0.52
P48-5	Qtz vein in bleached gneiss	52	30	70	20	27.0	161,000	1,150	b.d.	1,330	317	-0.88
P54-5	Qtz vein in fresh gneiss	64	55	45	19	29.8	180,000	475	b.d.	206	852	-0.47
P70-1	Qtz+dol+hem+drv breccia	122	100	0	18	28.4	171,000	449	b.d.	326	860	0.79
P-Patch deposit - Dolomite veins												
P48-3Dol	Qtz-dol vein in chloritized gneiss	40	0	100	17	28.0	169,000	1,290	b.d.	b.d.	295	-0.45

TABLE 2 (continued)

Sample	Description	Depth below U/C (m)	FI frequency (%) NaCl-rich brine	FI frequency (%) $CaCl_2$-rich brine	*N*	Av. salinity wt% eq. NaCl	Cl (ppm)	Br (ppm)	F (ppm)	SO_4 (ppm)	Cl/Br (molar)	$\delta^{37}Cl$ (‰)
Rabbit Lake deposit - Quartz veins												
DDH197-2	Qtz vein in albitized gneiss	21.6	70	30	10	30.2	182,000	1,340	b.d.	b.d.	306	-0.3
DDH7-1	Qtz filling vugs in dequartzified gneiss	125.5	15	85	18	29.6	178,000	409	b.d.	938	981	n.d.
RBL3Qz	Qtz cementing chl-drv breccia	n.d.	30	70	46	28.1	169,000	1,490	185	b.d.	255	-0.4
RBL4Qz	Qtz+dol vein in gneiss	n.d.	35	65	11	28.7	173,000	667	b.d.	375	585	-0.18
RBL2Qz	Qtz+dol vein in gneiss	n.d.	100	0	48	29.2	174,000	1,810	b.d.	2,010	216	n.d.
RBL7Qz	Qtz+dol vein in hydraulic megabreccia	n.d.	55	45	9	28.9	174,000	1,350	b.d.	b.d.	291	-0.12
RBL14Qz	Qtz+dol vein in gneiss	n.d.	100	0	16	29.0	175,000	581	b.d.	b.d.	680	-0.26
RBL5Qz	Qtz+dol vein in hydraulic megabreccia	n.d.	45	55	62	29.7	177,000	2,620	b.d.	356	152	-0.44
RBL9Qz	Qtz+dol vein in gneiss	n.d.	60	40	10	31.3	186,000	2,770	b.d.	1,000	151	n.d.
Rabbit Lake deposit - Dolomite veins												
RBL2Carb	Qtz+dol vein in gneiss	n.d.	100	0	40	27.6	158,000	1,560	b.d.	8,200	227	-0.19
RBL14Carb	Qtz+dol vein in gneiss	n.d.	20	80	19	27.2	161,000	1,160	b.d.	2,920	311	n.d.
RBL5Carb	Qtz+dol vein in hydraulic megabreccia	n.d.	0	100	11	27.4	162,000	2,860	105	1,650	127	-0.85
DDH197-5	Dol+chl vein in gneiss	n.d.	40	60	20	27.3	162,000	1,680	b.d.	1,210	218	0.05
RBL9Carb	Qtz+dol vein in gneiss	n.d.	35	65	15	27.3	163,000	1,810	b.d.	708	202	n.d.
RBL11Carb	Dol on bleached gneiss	n.d.	35	75	16	28.0	168,000	749	b.d.	1,250	504	-0.24
RBL7Carb	Qtz+dol vein in hydraulic megabreccia	n.d.	90	10	17	28.1	168,000	2,250	b.d.	b.d.	168	-0.04
RBL1Carb	Qtz+dol vein in gneiss	n.d.	100	0	17	28.5	170,000	2,030	b.d.	1,520	188	-0.12
Rabbit Lake deposit - Calcite veins												
RBL12Carb	Massive cal in gneiss	n.d.	0	100	15	28.9	172,000	2,770	b.d.	b.d.	140	n.d.
Millennium deposit - Quartz veins												
CX52-1	Qtz+dol vein in bleached gneiss	99	55	45	24	29.2	176,000	1,100	b.d.	b.d.	360	-0.43
CX48-03	Qtz+drv vein in bleached gneiss	130	20	80	17	28.1	170,000	1,150	b.d.	b.d.	333	0.36
CX44-2	Qtz vein in fresh gneiss	213	20	80	17	28.0	169,000	981	b.d.	b.d.	388	-0.22
CX48-01-12a	Qtz vein in hematized gneiss	265	0	100	2	28.0	169,000	428	b.d.	b.d.	892	-0.06

TABLE 2

Alteration	Sample	Cl (ppm)	L.O.I. (wt.%)
	Eagle Point porphyry granite		
Fresh	EPE-44-15	215	1.2
	EPE-44-12	436	1.4
	EPE-44-16	343	1.7
Altered	1935-10-b	198	1.5
	EPE-44-6	106	1.8
	1935-17	153	2.2
	EPE-44-1	112	3.0
	EPE-44-5	106	3.0
	EPE-44-9	195	3.8
	EPE-44-8	158	3.9
	1935-3	127	4.0
	EPE-44-2	207	4.5
	1935-4	91	4.6
	1935-11	271	5.1
	1935-7	132	5.4
	EPE-44-3	203	5.5
	1935-6	118	5.8
	P-Patch pegmatite		
Fresh	P56-53	883	1.2
	P60-1	518	1.2
	P62-17	1,078	1.4
	P62-19	460	1.7
Altered	P57-3	137	1.9
	P57-1	185	3.1
	P62-18	92	3.2
	P58-19	114	3.3
	P56-6	298	3.9
	P56-7	220	3.9
	P56-62	110	4.1
	P56-12	282	4.3
	P58-18	67	5.2
	P57-10	113	5.9
	P58-16	73	7.7
	P58-13	80	9.4

Mineral	Cl (ppm) (average)	*N*
	Eagle Point porphyry granite	
Biotite	3,250 to 4,170 (3,850)	18
Illite	210 to 340 (285)	4
Sudoite	250 to 530 (364)	9

1

2 TABLE 3

3